AFOSR 70-2780TR

THE INVERSE SCATTERING AND TARGET IDENTIFICATION PROBLEM

K.J. Breeding and A.A. Ksienski

AD717747

The Ohio State University

ElectroScience Laboratory

Department of Electrical Engineering
Columbus, Ohio 43212

TECHNICAL REPORT 2768-4

4 November 1970

Contract No. AFOSR 69-1710A

Department of the Air Force
Air Force Office of Scientific Research
Arlington, Virginia 22209

NOTICES

When Government drawings, specifications, or other data are used for any purpose other than in connection with a definitely related Government procurement operation, the United States Government thereby incurs no responsibility nor any obligation whatsoever, and the fact that the Government may have formulated, furnished, or in any way supplied the said drawings, specifications, or other data, is not to be regarded by implication or otherwise as in any manner licensing the holder or any other person or corporation, or conveying any rights or permission to manufacture, use, or sell any patented invention that may in any way be related thereto.

THE INVERSE SCATTERING AND TARGET IDENTIFICATION PROBLEM

K.J. Breeding and A.A. Ksienski

TECHNICAL REPORT 2768-4

4 November 1970

Contract No. AFOSR 69-1710A

Department of the Air Force
Air Force Office of Scientific Research
Arlington, Virginia 22209

CONTENTS

THE INVERSE SCATTERING AND TARGET IDENTIFICATION PROBLEM

K.J. Breeding and A.A. Ksienski

I. INTRODUCTION

In order to obtain an exact solution to the inverse scattering problem, the target response is required over a continuous band of frequencies and aspect angles.[1] An alternative approach to the problem which requires a much more modest amount of measurement data but assumes substantial a priori information is as follows: A finite set of alternatives is specified regarding target shape and composition and a set of measurements is carried out to provide the answer as to which one of the alternatives holds. Since it is necessary to restrict the measurements to a relatively small range of frequencies the question arises as to what frequency band is best to characterize the target and to provide the most reliable discrimination from other targets. The best apparent choice is the highest frequency possible since for a given per cent bandwidth it would contribute the greatest amount of information. Also, the high frequencies provide the resolution which yield fine detail. The high frequency approach has been the most widely accepted approach for obtaining target signatures. However, an examination of the Fourier transform of the impulse response indicated that the frequency range corresponding to wavelengths starting with the size of the object and increasing to ten times its dimension would provide the most useful initial information.[2,3] At higher frequencies the responses of various objects appear to be less typical of any specific object. This explains the failure of the "target signature" approach where the scattering cross sections were examined mostly at high frequencies. This does not imply that the upper end of the spectrum is not useful for the characterization of objects, however it must be utilized in conjunction with the lower frequency response to provide a meaningful description. The higher frequencies characterize the finer detail of the object while the lower frequencies provide the gross detail such as overall dimensions, approximate shape, and material. Obviously presenting only fine detail yields a rather confusing picture.

It is the low frequency range which is used in this paper to characterize the various objects of interest, and provides the information used to identify the objects, i.e., to choose the alternative which is most likely to be true. The term "likelihood" rather than "certainty" is used because of the incomplete knowledge of the target response as represented by a limited frequency and aspect angle sampling and, of course, due to noise and measurement errors. To determine whether the various targets of interest can be reliably identified based on the proposed low frequency characterization it must be shown that each target is represented in nonoverlapping regions of an appropriate space, such that when a certain set of radar measurements have been made a decision could be reached with regard to the target and that such decision would have a high probability of being correct.

The specific set of frequencies chosen to illuminate the target are 12 harmonically related frequencies in the Rayleigh and first resonance region. The range of aspect angles has been as complete as possible to provide the most comprehensive representation of the object. The radar returns provide both phase and amplitude information which would yield a 24 dimensional vector which could then represent each aspect angle of the object. The set of points, in such a 24 dimensional space, corresponding to the various aspect angles would then delineate the region of the space which would characterize the particular object and hopefully would do it uniquely, i.e., without overlapping a region corresponding to another object. Although, as mentioned, the phase information is available, it was decided to utilize only the amplitudes of the radar returns. The reason for this decision is that to date no satisfactory method has been found to remove the sensitivity of the phase data to range, and since the fundamental properties of class separability was investigated data with large potential for errors were considered undesirable.

Thus, each object was represented by a set of real 12-tuples $x = (x_1, x_2, \cdots, x_{12})$ each element of which corresponded to the magnitude of the return signal at the frequency 30i MHz (where $i = 1, \cdots 12$). There is, of course, one such vector for each aspect angle associated with the objects in question.

Various aspects of target classification utilizing the above spectral representation have been studied. In Section II the linear separability of the various classes is considered. Section III presents a specific approach for the design of an automatic target classifier and its performance is tested for various objects in the presence of noise and errors. Section IV discusses adaptive procedure for target classification. Section V presents a method for identification of target dynamics and, finally, Section VI considers the use of nonlinear decision surfaces for the target classification.

II. LINEAR SEPARABILITY OF OBJECT CLASSES

Since the data is represented as a set of real 12-tuples for each object, the possibility exists of attempting a linear separation of classes in 12 space. In general such linear separation may be described as follows. Let $S = \{\sigma_1, \sigma_2, \cdots, \sigma_r\}$ be a set of r objects to be classified. Associated with each object $\sigma_i \epsilon S$ is a set of n-tuples (in our case, 12-tuples), $A\sigma_i$. Without loss of generality, define the sets

(1) $$A = A\sigma_1$$

and

(2) $$B = \bigcup_{j=2}^{p} A\sigma_j, \quad 2 < p \leq r.$$

The sets A and B are said to be linearly separable if, and only if, there exists a hyperplane, H, characterized by the separating vector, $[\omega_1, \omega_2, \cdots, \omega_n; T] = [\vec{\omega}; T]$ such that

(3) $$\vec{\omega} \cdot \vec{a}^{(j)} \geq T, \quad \text{for all } a^{(j)} \; \epsilon \; A$$

and

(4) $$\vec{\omega} \cdot \vec{b}^{(j)} < T, \quad \text{for all } \vec{b}^{(j)} \; \epsilon \; B,$$

where $\vec{\omega} \cdot \vec{x}$ denotes the inner product of vectors $\vec{\omega}$ and $\vec{x}$.

In general measurement errors and other forms of noise may be introduced into the data. Since a solution to (3) and (4) consists of determining a real vector $\vec{\omega}$ and a real number T such that these inequalities are satisfied, any small error in new data may place the resulting point on the wrong side of the hyperplane. To reduce the effects of minor variations in data due to noise or measurement errors, it is desirable to have no points in the original training sets, A and B, fall on the hyperplane. This objective may formally be handled by reformulating the original problem as

(5) $\vec{\omega} \cdot \vec{a}^{(j)} \geq T + \delta$, for all $\vec{a}^{(j)} \in A$

and

(6) $\vec{\omega} \cdot \vec{b} \leq T - \delta$, for all $\vec{b}^{(j)} \in B$

where δ is an arbitrarily small positive real number. These inequalities may be normalized by dividing through by δ and replacing $\vec{\omega}$ by $\vec{\omega}/\delta$ and T by T/δ. In so doing the initial problem of determining the separating vector $[\vec{\omega}; T]$ from the original training sets may be reformulated as

(7) $\vec{\omega} \cdot a^{(j)} \geq T + 1$, for all $\vec{a}^{(j)} \in A$

and

(8) $\vec{\omega} \cdot \vec{b}^{(j)} \leq T - 1$, for all $\vec{b}^{(j)} \in B$.

Problems of the type given by inequalities (7) and (8) will, of course, have an infinity of solutions if one exists at all. There are many ways of solving problems formulated as in (7) and (8). One particularly appropriate procedure which determines a specified solution, assuming one exists, is that of linear programming.[4] In this approach inequalities (7) and (8) are solved subject to the condition that some linear form is to be minimized. It has been shown[5] that the reliability of a threshold device used to realize a linear classifier is increased if the value of T in (7) and (8) is minimized. Thus, the objective function of minimizing T subject to the constraints imposed by (7) and (8) forms the required linear programming problem.

Results

Referring to the original backscatter data it will be observed that this original data, which forms the training sets, consisted of 10 points representing the prolate spheroid (P.S.), 10 points for the cube (c), 5 points for the hemispherical boss (HSB), 3 sphere points (S), and 2 points for the wire. To investigate the possibility of linear separability, hyperplanes were found based on the formulation in (7) and (8) which separated each object from all the others. The somewhat unexpected result was that this was possible. The resulting hyperplane direction numbers are shown in Table I. Two rather interesting observations may be made. First, note that in each case $T = 0$. This, of course, means that the respective separating hyperplane passes through the origin. The physical reason for this is not at present clear. The second observation is that $\omega_1 = 0$ in all cases. It has been conjectured [2] that this component, which corresponds to the first resonant peak, is in some way indicative of the overall size of the target. Since each of the objects considered were roughly of the same size, this first resonant peak would then appear at about the same frequency in each case. Thus, this component can play no part in the overall separation.

Since each of the objects is separable from all others taken together, they must be pairwise separable. These pairwise separating hyperplanes were next calculated and their parameters are given in Table II. It should be observed once again that T = 0, $\omega_1 = 0$, as would be expected from the results shown in Table I. These pairwise separating hyperplanes are used later as a basis for an automatic classification procedure. One further comment should be made here. Each occurrence of a zero in Tables I and II implies that there exists some characteristic similarity between the classes of objects in question and indicates that other dimensions are more effective in the identification of the object. Exactly what these similarities may be due to is not, at this time, known.

Since only a relatively few number of points were used to determine the separating hyperplanes, it is fair to wonder whether separation is maintained for data obtained at different aspect angles than used initially. To this end, the data for the cube, hemi-spherical boss, and prolate spheroid were interpolated to produce data at 1° increments in aspect angle. The interpolation procedure used is discussed in detail in Appendix A. These interpolated data were then compared with each of the hyperplanes of Table II with the result that the separation specified by inequalities (7) and (8) was maintained. This fact indicates that the data representations taken for the objects is apparently quite indicative of the objects and further that these points must strongly cluster in the Euclidian 12 space, E_{12}.

TABLE I

TOTAL SEPARATING HYPERPLANES

	C.	S.	P.S.	H.S.B.	W
ω_1	0	0	0	0	0
ω_2	-157.91	-113.46	11.54	0	-5.78
ω_3	136.42	83.1	0	-176.55	-7.09
ω_4	-46.32	0	-2.78	0	7.54
ω_5	0	-37.33	0	0	0
ω_6	-5.97	0	0	0	16.5
ω_7	0	12.57	-4.34	0	-38.06
ω_8	0	-199.72	0	165.48	6.86
ω_9	6.66	60.71	-4.35	0	0
ω_{10}	0	-109.93	0	0	27.49
ω_{11}	0	236.56	0	0	-18.94
ω_{12}	-4.29	0	0	0	0
T	0	0	0	0	0

TABLE II

PAIRWISE SEPARATING HYPERPLANES

	PS/S	PS/HSB	PS/C	PS/ω	S/HSB	S/C	S/ω	HSB/C	HSB/ω	C/ω
ω_1	0	0	0	0	0	0	0	0	0	0
ω_2	11.98	0	3.54	0	0	0	0	0	0	0
ω_3	0	8.36	0	9.04	-4.8	0	0	0	0	25.89
ω_4	-9.13	0	-2.29	-1.92	0	-8.63	0	-7.91	-64.85	0
ω_5	0	0	0	0	19.89	0	0	0	0	-20.48
ω_6	0	0	0	0	0	0	0	0	0	0
ω_7	0	0	0	0	0	0	0	0	0	-15.68
ω_8	0	-7.57	-.35	0	0	-6.34	0	6.94	0	0
ω_9	0	0	.23	-8.05	0	-.49	-16.52	0	16.56	5.36
ω_{10}	0	4.49	0	0	0	0	0	-3.61	0	0
ω_{11}	0	0	0	0	0	0	0	0	0	0
ω_{12}	0	0	0	0	-5.69	12.97	12.59	0	0	0
T	0	0	0	0	0	0	0	0	0	0

As was mentioned earlier, the inequalities (3) and (4) were modified to inequalities (7) and (8) as an attempt to reduce the effect of noise on the identification of the objects. To examine the consequences of this modification, two experiments were performed on the data for the prolate spheroid, the three spheres, and five of the cube data points. In the first experiment uniformly distributed noise bounded in absolute value by a constant, a, was added to the elements of the cube and sphere backscatter data. New separating hyperplanes were then computed based on inequalities (7) and (8). The results of these experiments are given in Table III where the signal to noise ratio, S/N, is based on the average return signal amplitude and the average of the absolute value of the applied noise. The first observation to be made from this data is that the general topology of the points in E_{12} are not appreciably affected by the addition of noise whose average level is significantly below that of the signal. This is indicated by the fact that the resulting hyperplanes are only slightly varied from their original positions up to an S/N of 19 dB. However, when the S/N becomes - 1dB the situation changes considerably. First, interestingly enough, the sets of points are linearly separable but the separating hyperplanes orientation has been considerably altered from the no noise situation. These results thus, indirectly reinforce the choice for inequalities (7) and (8).

In the second experiment noise in the same steps as for Table III was added to the sphere, cube, and prolate spheroid data. The relative distance, $\vec{\omega} \cdot \vec{x}$, from the sphere/cube hyperplane was then computed. These computations are based, effectively, on inequalities (3) and (4). This data is shown in Table IV. In this table a positive number means

TABLE III

SPHERE/CUBE HYPERPLANES WITH NOISE ADDED TO RETURN SIGNAL

	S/N	36 dB	19 dB	-1 dB	19 dB
	No Noise	.01≥|noise| S.only	.1≥|noise| S.only	1≥|noise| S.only	.1≥|noise| C S
ω_1	0	0	0	0	0
ω_2	0	0	0	0	0
ω_3	.5	.41	.27	0	.26
ω_4	0	0	0	.06	0
ω_5	0	0	0	1.46	0
ω_6	4.72	4.84	7.21	0	6.99
ω_7	0	0	0	-.57	0
ω_8	-3.35	-3.28	-3.94	-1.46	-4.27
ω_9	1.32	1.26	1.26	1.04	1.94
ω_{10}	0	0	0	0	0
ω_{11}	0	0	0	0	0
ω_{12}	0	0	0	0	0
T	0	0	0	0	0

TABLE IV

RELATIVE DISTANCE OF NOISY POINTS FROM SPHERE/CUBE HYPERPLANE

S/N / Points	No noise	36 dB	19 dB	-1 dB
S1	1.0	1.03	.65	3.27
S2	3.49	3.44	3.43	-2.45
S3	1.0	.98	.6	3.33
C1	-1.0	-.97	-.69	3.34
C2	-1.27	-1.32	-1.79	6.78
C3	-1.0	-1.02	-1.23	-.24
C4	-1.04	-1.07	-1.39	.03
C5	-1.5	-1.51	-1.56	-5.29
PS1	2.05	2.08	1.54	.96
PS2	2.36	2.31	2.0	5.35
PS3	3.22	3.19	2.82	3.07
PS4	4.36	4.32	5.19	7.02
PS5	4.06	4.06	3.52	.26
PS6	1.76	1.72	1.76	1.83
PS7	.5	.52	.64	-2.75
PS8	.77	.71	.72	6.34
PS9	1.94	1.96	1.59	4.42
PS10	2.57	2.65	2.38	3.51

the data point is above the hyperplane." Notice from this table, that no points are misclassified until the S/N becomes about - 1 dB. This fact confirms the observations made from the data of Table III and justifies the decision to determine the separating hyperplanes from the training data based on inequalities (7) and (8). Notice one further thing in Table IV, that the sphere and the prolate spheroid data are located on the same side of the sphere/cube hyperplane. This result might have been anticipated from the fact that these two objects, spheres and prolate spheroids, are geometrically quite similar.

III. AUTOMATIC TARGET CLASSIFICATION BASED ON SPECTRAL RESPONSE

The result that the classes of objects studied above are linearly separable suggests a possible scheme for automatically identifying targets. Let

$$S = \{\sigma_1, \cdots, \sigma_r\}$$

be the set of r object classes with each object represented by the training set

$$A\sigma_i = \left\{\vec{a}^{(i,1)}, \vec{a}^{(i,2)}, \cdots, \vec{a}^{(i,\alpha_i)}\right\}, \; i = 1, 2, \cdots, r$$

of n-tuples. In accordance with the results of Section II assume that every pair of object sets, $A\sigma_i$ and $A\sigma_j$, are linearly separable by the hyperplane $H_{i,j}$. Each such hyperplane is represented by a separating vector $[\vec{\omega}^{(i,j)} \cdot T_{i,j}]$ such that

$$\text{(9)} \qquad \vec{\omega}^{(i,j)} \cdot \vec{a}^{(i,k)} \geq T_{ij} + 1 \text{ for all } \vec{a}^{(i,k)} \in A\sigma_i$$

and

$$(10) \qquad \vec{\omega}^{(i,j)} \cdot \vec{a}^{(j,\ell)} \leq T_{ij} - 1 \text{ for all } \vec{a}^{(j,\ell)} \in A\sigma_j \; .$$

Thus, inequalities (9) and (10) determine a separating hyperplane for any pair of training sets $A\sigma_i$ and $A\sigma_j$. Since there are r classes of objects and since $\vec{\omega}^{(i,j)} = -\vec{\omega}^{(j,i)}$ and $T_{i,j} = -T_{j,i}$, from (9) and (10), for $i \neq j$, $i,j = 1, \cdots r$ there will be $r(r - 1)/2$ distinct hyperplanes. These hyperplanes may now be used to identify objects in the set S or to help in the classification of new objects on data which was not in the original training sets.

Assume that the hyperplane $H_{i,j}$ have been determined from the training sets. Further assume that an unknown object $\chi \varepsilon S$ is the target and let

$$B = \left\{ \vec{x}^{(1)}, \vec{x}^{(2)}, \dots, \vec{x}^{(3)} \right\}$$

be a set of points characterizing χ. The objective now is to attempt an identification of χ as one of the $\sigma_i \varepsilon S$. For each $\vec{x}^{(k)} \varepsilon B$ a tentative classification of that point into catagory σ_i may be made on the basis of the inequality

$$(11) \qquad \vec{\omega}^{(i,j)} \cdot \vec{x}^{(k)} > T_{i,j}, \; i \neq j, \; j = 1, 2, \cdots r.$$

This criteria is used for two purposes. One is to avoid any ambiguity arising due to noise on the data and the other is to classify only those data which lie above and not on the test hyperplane.

Any point satisfying (11) will go into catagory σ_i and any point lying on the hyperplane in question should properly be ignored. This may be done by defining the following. Let

$$(12) \qquad \delta_{ij}^{(k)} = \begin{cases} , \text{ if } \vec{\omega}^{(i,j)} \cdot \vec{x}^{(k)} - T_{i,j} > 0 \\ 0 \text{ otherwise} \end{cases}$$

and let

$$(13) \qquad \rho_i^{(k)} = \sum_{\substack{j=1 \\ j \neq i}}^{1} \delta_{ij}^{(k)} \quad .$$

The metric $\rho_i^{(k)}$ thus defines the number of times the point $\vec{x}^{(k)}$ fell on the c_i side of the hyperplanes separating σ_i from the other $r - 1$ classes of objects. Clearly if $\rho_i^{(k)} = r - 1$ then $\vec{x}^{(k)}$ could, with a high degree of certainty, be classed as representing some view of the object σ_i. In general, however, $\rho_i^{(k)} \leq r - 1$ and, in fact, $\rho_\ell^{(k)} \neq 0$, $\ell \neq i$, for the general case. If $\chi = \sigma_i$ then $\rho_i^{(k)} \geq \rho_\ell^{(k)}$ for all k and $i \neq \ell$. Since it is desirable to class each $\vec{x}^{(k)}$ into one of the classes of r catagories it is desirable to have some metric which indicates the proportionate classifications of each of the object points. Thus, define

$$(14) \qquad C_i^{(k)} = \begin{cases} \dfrac{\rho_i(k)}{r - 1} \quad , \quad \rho_i^{(k)} = \underset{j-1,\cdots,r}{\text{Max}} (\rho_j^{(k)}) \\ 0 \qquad \text{otherwise} \quad . \end{cases}$$

From (14) a final metric representing all of the data in B may be defined as

$$(15) \qquad C_i = \frac{\sum_{k=1}^{S} C_i^{(k)}}{S} \quad .$$

It should be noted that $\sum_{i=1}^{S} C_i$ is not in general equal to one, and, thus, cannot be construed as a probability of classification. They are, however, closely related to the probability of classification with the main discrepancy due to the vanishing of some of the distances. If none of the points fall on the plane itself the sum of C_i would, indeed, be unity. Thus, the value of C_i is bounded from above by the probability measure, hence, it is a conservative measure. For example, if $C_i = .8$ it can be deduced that at least 80% of the points of set B fell on the σ_i side of the hyperplane. In the experiment to be described below, if the data points $A\sigma_i$ are introduced into the classifier and the result is $C_i = .8$ the conclusion may be drawn that the conditional probability or the likelihood function $p(C_i/A\sigma_i) \geq .8$; that is the probability of the object being classified correctly is at least 80%.

The experiment carried out utilized the pairwise separating hyperplanes given in Table II. However, the test data used were obtained by interpolation of the original training data for look angles which were not previously measured or computed (see Appendix A for the interpolation method), they constituted, therefore, an appropriate test set. In addition, noisy data were used to test the ability of the classifier to operate on data contaminated by various amounts of noise or measurement errors. Finally a set of data representing an object not previously included in the classification, namely a cylinder, were tested. The experimental data used are described below with the final metric of equation (15) given for each of these experiments in Table V. The notation used here is simplified to denote only the object class, σ_i, for which the metric C_i is a representative. The experiments performed are as follows.

1. Interpolated cube data for $\phi = 45°$, $\theta = 15°, 16°, \cdots 24°$, and $\hat{\phi}$ polarization with 10 points in the sample set.
2. Interpolated cube data for $\phi = 0°$, $\theta = 0°, 1°, 2°, \cdots, 9°$ and $\hat{\phi}$ polarization with 10 points in the sample set.
3. Interpolated data for hemi-spherical boss for $\theta = 15°, 16°, 17°, \cdots, 24°$ and $\hat{\phi}$ polarization with 10 points in sample set.
4. Interpolated prolate sphere data for $\theta = 16°, 17°, 18°, 19°$ and $\hat{\phi}$ polarization with 4 points in sample set.
5. Original prolate spheroid data with noise added to produce S/N = 36 dB.
6. Same as 5 except that the noise added produced S/N = 19 dB.
7. Same as 5 except that the noise added produced S/N = -1 dB.
8. Five points of the original cube data for $\phi = 0$, $\theta = 0, 15, 30, 45$, and $\phi = 45$, $\theta = 15$ with noise added to produce S/N = 36 dB.
9. Same as 8 except that the noise added produced S/N = 19 dB.
10. Same as 8 except that the noise added produced S/N = -1 dB.
11. Original three sphere data point with noise added to produce an S/N = 36 dB.
12. Same as 11 except that the noise added produced an S/N = 19 dB.
13. Same as 11 except that the noise added produced an S/N = -1 dB.

TABLE V

EXPERIMENTAL RECOGNITION RESULTS
AS INDICATED BY THE PARAMETER C_i

Test	PS	S	HSB	C	W
1	0	0	0	1.0	0
2	0	0	0	1.0	0
3	0	0	1.0	0	0
4	1.0	0	0	0	0
5	1.0	0	0	0	0
6	1.0	0	0	0	0
7	.7	0	0	.1	.15
8	0	0	0	.8	.15
9	0	.2	0	.6	.15
10	0	0	0	.4	.5
11	0	1	0	0	0
12	0	.667	0	.333	0
13	.333	0	0	.333	.333
14	.7	0	0	0	.225
15	.1	0	0	0.1	.65

14. Ten points representing a right circular cylinder having a diameter of D = .635 m and length L = 1.27 m oriented along the Z axis for $\theta = 0°, 10°, 20°, \cdots, 90°$ and $\hat{\theta}$ polarization.

15. The same cylinder as described in 14 but with $\hat{\phi}$ polarization of illuminating signal.

First it may be noted that the interpolated test set experiments 1-4 were classified without any errors. The classification of the prolate spheroid is highly reliable even in the presence of noise. As experiments 5-7 indicate no errors occurred up to S/N of 19 dB and even at S/N = - 1 dB the probability of correct classification was no less than 70%. The cube and sphere classification was less resistant to noise (experiments 8-13), however, when wrong classifications were made the reliability factor was indicated as very low, for example, when the sphere was classified as a cube, wire or prolate spheroid, it was indicated that the choices carried only about 30% reliability, stressing the need for further data to obtain a more reliable decision. Whenever the reliability indicator C_i exceeded 60% the choice was found to be correct.

The last two experiments are of particular interest. Consider experiment 15 first. Here a right circular cylinder was illuminated in the same way that the thin wire (itself a cylinder of dimensions D = .05 m and L = 1 m) was illuminated. The .65 in Table 5 experiment 15 indicates very strongly the obvious connection between the wire and the cylinder. In experiment 14, on the other hand, the polarization was along the illumination axis or $\hat{\theta}$. The identification for this case resulted in the cylinder appearing as a prolate spheroid. There is a striking similarity here. The ratio of the length to diameter of the cylinder, 2, is the same as the ratio of the major axis to minor axis of the prolate spheroid. Further if the discontinuities of the cylinder were removed a prolate spheroid could easily be produced. These facts tend to reinforce the opinion that the spectral response data tends to cluster in 12 space in accordance with the general size and shape of the target object.

IV. ADAPTIVE DETERMINATION OF LINEAR SEPARATING HYPERPLANES

The solution of the inequalities (7) and (8) may be handled in a number of ways. One of which is the simplex method of linear programming which was used in the previous sections. The main difficulty with this procedure is that it is generally unable to handle new or modified data sets. It has been shown,[6] however, that suitable modifications of linear programming algorithms can produce adaptible linear classifiers. There are, of course, many other algorithms applicable to adaptive linear classification.[7,8,9] In all of these algorithms the speed of convergence and the amount of computation is generally quite large.

Adaptive algorithms generally proceed by estimating a separating hyperplane and then making a new estimate based on an observation of the system with the first estimate. The change, generally, is dictated by the data which is incorrectly classified. The method by which each new estimation of separating hyperplanes is made has a great deal to do with the rapidity of convergence as, also, does the initial hyperplane estimate.

Let A and B be two sets of n-tuples in Euclidean n space, E_n. If A and B are linearly separable, then there exists a real vector $\vec{\omega}$ and a real number T such that

$$(16) \qquad \vec{\omega} \cdot \vec{a}^{(i)} \geq T, \qquad \vec{a}^{(i)} \varepsilon A$$

$$(17) \qquad \vec{\omega} \cdot \vec{b}^{(j)} < T, \qquad \vec{b}^{(j)} \varepsilon B.$$

The problem now is to determine the $\vec{\omega}$ and T. Consider Fig. 1. A reasonable approximation to the first hyperplane may be made based on the location of the center of gravities of each set A and B. In particular let

$$(18) \qquad \vec{p}_A{}^{(o)} = \frac{1}{r} \sum_{i=1}^{r} \vec{a}^{(i)}$$

$$(19) \qquad \vec{p}_B{}^{(o)} = \frac{1}{s} \sum_{i=1}^{s} \vec{b}^{(i)}$$

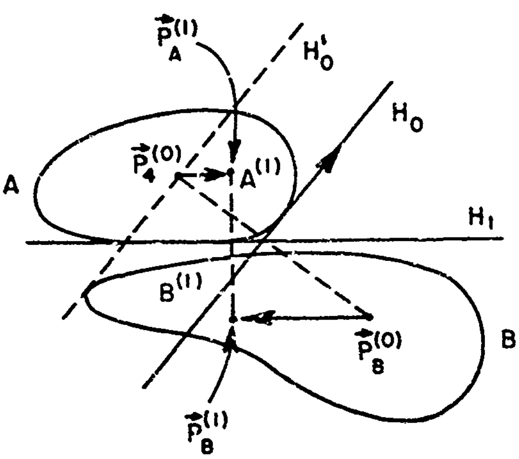

Fig. 1. Illustration of the adaptive procedure.

where r and s are the orders of sets A and B respectively. Then as an initial estimate of the separating vector let

$$(20) \qquad \vec{\omega}^{(o)} = \vec{p}_A^{(o)} - \vec{p}_B^{(o)}$$

and

$$(21) \qquad T_o = \underset{i}{\mathrm{Min}} \left(\vec{\omega}^{(o)} \cdot \vec{a}^{(i)}\right), \qquad \vec{a}^{(i)} \in A.$$

This hyperplane is shown in Fig. 1 and is labeled H_o. If all of the vectors in B satisfy (17) then clearly this choice is an admissible separating hyperplane. Assume, however, that this is not the case. Let

$$B^{(1)} = \left\{\vec{b}^{(j_1)}, \vec{b}^{(j_2)}, \cdots, \vec{b}^{(j_{\beta_1})}\right\} \subseteq B$$

be the set of vectors which do not satisfy inequality (17). The problem becomes one of moving the hyperplane so that these vectors will be correctly separated. Referring to Fig. 1, if the point $\vec{p}_B^{(o)}$ were moved in the general direction of the set of vectors $B^{(1)}$ then the hyperplane H_o, which is perpendicular to the line joining $\vec{p}_A^{(o)}$ and $\vec{p}_B^{(o)}$ would be "tipped" in the right way to bring, hopefully, some of the incorrectly separated vectors to the correct side of the hyperplane. It turns out, however, that under some conditions this procedure will produce a hyperplane which is a worse approximation than the first estimate.

To avoid this situation define the hyperplane H_o' as one parallel to H_o but with a T_o' defined as

$$(22) \qquad T_o' = \underset{j}{\mathrm{Max}} \left(\vec{\omega}^{(o)} \cdot \vec{b}^{(j)}\right), \qquad \vec{b}^{(j)} \in B \quad .$$

Thus, for H_o', inequalities (17) are satisfied for all $\vec{b}^{(j)} \in B$ but inequalities (16) will not, in general, be satisfied for all $\vec{a}^{(i)} \in A$. Let

$$A^{(1)} = \left\{\vec{a}^{(i_1)}, \vec{a}^{(i_2)}, \cdots, \vec{a}^{(i\alpha_1)}\right\} \subseteq A$$

be the set of vectors in A which do not satisfy inequalities (16) under hyperplane H_o'. Using this information point $\vec{p}_A^{(o)}$ may be moved in the general direction of the set $A^{(1)}$ and $\vec{p}_B^{(o)}$ may be moved in the direction of the set $B^{(1)}$. Thus, define

$$(23) \qquad \vec{p}_A^{(1)} = \left(\vec{r}\, p_A^{(o)} + \sum_{k=i_1}^{i\alpha_1} \vec{a}^{(k)}\right) / (r + \alpha_1)$$

and

$$(24) \qquad \vec{p}_B^{(1)} = \left(r\, \vec{p}_B^{(o)} + \sum_{k=j_1}^{j\beta_1} \vec{b}^{(k)}\right) / (r + \beta_1) \ .$$

A new hyperplane estimate may now be made based on these quantities as follows. Define

$$(25) \qquad \vec{\omega}^{(1)} = \vec{p}_A^{(1)} - \vec{p}_B^{(1)}$$

and

$$(26) \qquad T_1 = \underset{i}{\mathrm{Min}}(\vec{\omega}^{(1)} \cdot \vec{a}^{(i)}).$$

The resulting hyperplane is shown in Fig. 1 as H_1.

In this illustration H_1 succeeded in separating sets A and B. In general this may not happen. What is required in this case is to repeat the above procedure. In general each estimate may be defined as follows:

$$(27) \qquad \vec{\omega}^{(g)} = \vec{p}_A^{(g)} - \vec{p}_B^{(g)}$$

and

$$(28) \qquad T_g = \underset{i}{\mathrm{Min}}\, (\vec{\omega}^{(g)} \cdot \vec{a}^{(i)})$$

where

$$(29) \qquad \vec{p}_A^{(g)} = \frac{\left[\left(\sum_{j=0}^{g-1} \alpha_j\right) \vec{p}_A^{(g-1)} + \sum_{\ell=i_1}^{i_{\alpha_g}} \vec{a}^{(\ell)}\right]}{\sum_{j=0}^{g-1} \alpha_j + \alpha_g}$$

and

$$(30) \qquad \vec{p}_B^{(g)} = \frac{\left[\left(\sum_{j=0}^{g-1} \beta_j\right) \vec{p}_A^{\prime g-1)} + \sum_{\ell=i_1}^{i_{\beta_g}} \vec{b}^{(\ell)}\right]}{\sum_{j=0}^{g-1} \beta_j + \beta_g}$$

where $\alpha_0 = r$, $\beta_0 = S$ and α_j and β_j are the orders of the sets

$$(31) \qquad A^{(j)} = \left\{ \vec{a} \in A \;\middle|\; \vec{\omega}^{(i)} \cdot \vec{a} < T_j' = \operatorname*{Max}_i \left(\vec{\omega}^{(i)} \cdot \vec{b}^{(i)}\right) \right\}$$

and

$$(32) \qquad B^{(i)} = \left\{ \vec{b} \in B \;\middle|\; \vec{\omega}^{(i)} \cdot \vec{b} \geq T_j = \operatorname*{Min}_i \left(\vec{\omega}^{(j)} \cdot \vec{a}^{(i)}\right) \right\}$$

respectively.

This procedure was applied to some 40 different problems ranging in dimensionality from 2 to 5 variables. Among the problems which had the sets A and B consisting of binary n tuples (0's and 1's), the procedure converged for all problems in from 1 to 2 iterations.* The class of problems in which the vectors were arbitrary real numbers converged generally in from 3 - 4 iterations. One real vector problem required 79 iterations. Comparing these convergence rates with other procedures of a similar nature (cf references mentioned above) it was found that in all cases convergence was from 2 to 4 times faster than the other methods. Thus, the possibility of using this procedure for an adaptive identification procedure is certainly feasible.

---

* An iteration is defined here as a check of inequalities (16) and (17) for all vectors in A and B.

V. IDENTIFICATION OF TARGET DYNAMICS

Linear separability may be used for not only identifying target objects, as indicated above, but also as a method of inferring information concerning target dynamics. As an illustration of this process assume that the object $\sigma_i \in S$ has cylindrical symmetry and is the target object. Assume further that this object is rotating in some way in free space. At a set of discrete time intervals data is taken which represents the impulse response presented by σ_i at these time intervals.* Let this set of data be B. Then each $\vec{x}^{(k)} \in B$ represents the object as a function of its aspect angle in time.

Once the object represented by the data in the set B has been identified a real valued function of time, g(t), may be defined based on some separating hyperplane, H_{ij}, which separates data representative of σ_i from any other data set. Let this hyperplane have a separating vector of $[\vec{\omega}^{(i,j)}; T_{i,j}]$. Then g(t) may be defined as

$$(33) \qquad g(t) = \vec{\omega}^{(i,j)} \cdot \vec{x}(t) - T_{i,j}, \qquad \vec{x}(t) \in B.$$

This function represents the relative distance between the hyperplane, $H_{i,j}$, and the point $\vec{x}(t)$ which, in turn, is a function of aspect angle.

---

* It may be assumed here that the object is effectively motionless during the measurement interval.

At training time, a function of ψ, the aspect angle, may be generated based on the data in the training set $A\sigma_i$. For the case under consideration let this function be

$$(34) \qquad f(\psi) = \vec{\omega}^{(i,j)} \cdot \vec{a}^{(i,\ell)}(\psi) - T_{i,j}, \qquad \vec{a}^{(i,\ell)} \in A\sigma_i$$

$f(\psi)$ may reasonably be assumed to be a well behaved, continuous function of aspect angle. The aspect angle, ψ, is related to the spherical coordinates, θ and ϕ as shown in Fig. 2. From this figure

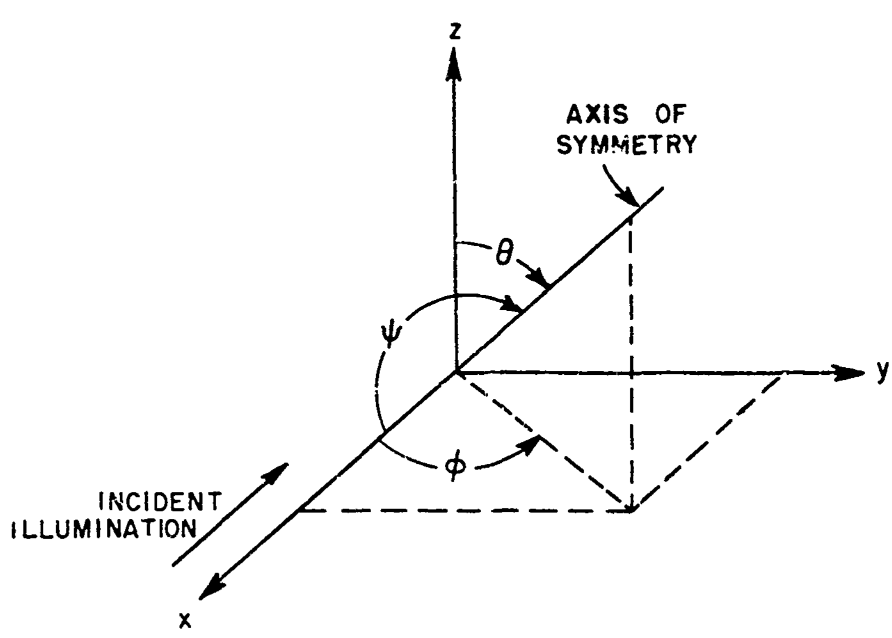

Fig. 2. Aspect angle of rotational axis of a cylindrical symmetrical object.

$$\psi = \cos^{-1} (\sin\theta \cos\phi). \tag{35}$$

In general both θ and ϕ are functions of time. Thus, if $g(t)$ can be related to $f(\phi)$ at each instant of time then $\psi(\tau)$ may be found and from (35) $\theta(t)$ and $\phi(t)$ may be inferred. This inference is, of course, not without ambiguity in the general case.

Consider as an example the following case. Let the object σ_i be rotating in space such that $\theta = \omega_0 t$ and $\phi = \phi_0$. Thus σ_i is rotating in a plane making an angle ϕ_0 with the direction of illumination. Thus, $\psi(t)$ becomes

$$\psi(t) = \cos^{-1} (\sin(\omega_0 t + \beta) \cos \phi_0), \tag{36}$$

where β is a phase angle produced by the time at which observations are begun.

Assume that during the observational period σ_i goes through at least one full revolution. Thus, the axis of symmetry must become co-linear with the z axis at least once. If this instant of time can be identified uniquely then ω_0 is found from the period of revolution and β becomes $\beta = - \omega_0 t_0$ where t_0 is the time at which $\psi(t_0) = 90°$. With this information at hand the value of ϕ_0 becomes simply

$$\phi_0 = \underset{t}{\mathrm{Min}} (\psi(t)). \tag{37}$$

Clearly this class of target dynamics is easily recognized. Other types of motion become more difficult to identify. This identification may, however, be made based on the training function $f(\psi)$ if a one to one correspondence between f( ) and g(t) can be found.

VI. NON LINEAR DECISION SURFACES

The application of separating hyperplanes to classify n-dimensional data, as was done above, may pose problems when the number of alternative objects is rather large. One, in particular, is that a single object classifier is not possible due to the necessity of having at least two sets of data to define a separating hyperplane. One data set is, of course, the set representing the target of interest. The second data set would thus, become that set representing all target objects which are not the chosen one - a most formidable array of data if the number of object classes is large.

A second difficulty has to do with updating the number of target classes. If a new target class is to be added to the set of k original classes then the addition will require determination of k new hyperplanes. Furthermore, this requires that the original data sets used for training be available for the addition of the new class.

One way of avoiding these difficulties is to use closed separating hypersurface such as "hyperboxes" and "hyperellipsoids." A hyperbox may be defined in n space, as a closed surface bounded by 2n hyperplanes such that each hyperplane is parallel to exactly one other hyperplane and perpendicular to the remaining 2n-2 hyperplanes. One particularly easy hyperbox to specify is one having its faces perpendicular to the coordinate axis. The position of each face along the axis is then determined by the maximum and minimum value of the corresponding component over the set of data. In particular, let

$$A = \{\vec{a}_1, \vec{a}_2, \cdots, \vec{a}_s\} ,$$

where

$$\vec{a}_i = (a_{i1}, a_{i2}, \cdots, a_{in})$$

be a set of data representing a particular target object. The hyperbox just described may now be specified by the two n-tuples

$$\vec{\omega}_M = (\omega_{M1}, \cdots, \omega_{Mn})$$

and

$$\vec{\omega}_m = (\omega_{m1}, \cdots, \omega_{mn})$$

where

$$\omega_{Mj} = \underset{i=1,\cdots,S}{\mathrm{Max}} (a_{ij})$$

and

$$\omega_{mj} = \underset{i=1,\cdots,S}{\mathrm{Min}} (a_{ij}).$$

Thus, a point $\vec{x}$ will be in the hyperbox if and only if

$$\vec{\omega}_m \leq \vec{x} \leq \omega_M$$

and thus, associated with the object whose training set is A. Although such an identification procedure is quite sim[illegible] it has a number of drawbacks. Not least of these is the very large volume of the hyperbox which does not contain any data points and thus, serves no useful classification purpose and, in fact, may contribute to erroneous classification.

To avoid such problems, it would appear that the volume of the enclosing hyperbox should be minimized in some sense. One way of specifying such a minimal hyperbox is to orient the faces a[illegible]g the axis of point "spread." This may be done in the following way. Let A be the set of training data and assume S, the number of points in A, to be not less than n, the space dimension. The first step in specifying the "minimal" hyperbox is to determine a hyperplane, H_1, which passes through the set of points in A and which is oriented along the axis of distribution of the points. Let this hyperplane be denoted by the weight vector (hyperplane normal) $\vec{\omega} = (\omega_{i1}, \omega_{i2}, \cdots, \omega_{in})$ and the real number T. More precisely this hyperplane is the one which minimizes

$$(38) \qquad z_1 = \sum_{i=1}^{S} \delta_{1i}^{\ 2}$$

where

$$(39) \qquad \delta_{1i} = \vec{\omega}_1 \cdot \vec{a}_i - T_1.$$

For z_1 to be minimized it is necessary that

$$(40) \qquad \frac{\partial z_1}{\partial \omega_{1j}} = 0, \; j = 1, 2, \cdots, n$$

and

$$(41) \qquad \frac{\partial z_1}{\partial T_1} = 0.$$

From (38) and (39)

(42) $$\frac{\partial z_1}{\partial \omega_{1j}} = 0 = 2 \sum_{i=1}^{S} a_{ij} \, (\vec{\omega} \cdot \vec{a}_i - T_1), \; j = 1, \cdots, n$$

and

(43) $$\frac{\partial z_1}{\partial T_1} = 0 = -2 \sum_{i=1}^{S} (\vec{\omega}_i \cdot \vec{a}_i - T_1).$$

From (43)

(44) $$ST_1 = \vec{\omega}_i \cdot \sum_{i=1}^{S} \vec{a}_i$$

or

(45) $$T_1 = \vec{\omega}_1 \cdot \vec{\rho}$$

where $\vec{\rho} = \frac{1}{S} \sum_{i=1}^{S} \vec{a}_i$ is the first moment of the set A.

The set of equations (42) form a homogeneous system of n equations in n unknowns since T_1 is dependent on $\vec{\omega}_1$ by (45). In order to determine a nontrivial solution, a constraint needs to be added to the system (42). One reasonable constraint is to assume that the sum of the weights and threshold is not zero or

(46) $$\vec{\omega}_1 \cdot \vec{I} + T_1 = k \neq 0$$

where

$$\vec{I} = (1, 1, \cdots, 1).$$

Thus, $T_1 = k - \omega_1 I$ and (42) becomes

$$0 = \sum_{i=1}^{S} 2\, a_{ij} \,(\vec{\omega}_1 \cdot \vec{a}_i - k + \vec{\omega}_1 \cdot \vec{I})$$

$$= 2\, \vec{\omega}_1 \cdot \sum_{i=1}^{S} a_{ij}\, (\vec{a}_i + \vec{I}) - 2\, k \sum_{i=1}^{S} a_{ij}$$

or

$$k \sum_{i=1}^{S} a_{ij} = \vec{\omega} \cdot \sum_{i=1}^{S} a_{ij}\, (\vec{a}_i + \vec{I}),\ j = 1, 2, \cdots, n. \tag{47}$$

In matrix form this becomes

$$\begin{bmatrix} b_1 \\ b_2 \\ \cdot \\ \cdot \\ \cdot \\ b_n \end{bmatrix} = \begin{bmatrix} C_{11} & C_{12} & \cdots & C_{1n} \\ C_{21} & C_{22} & \cdots & C_{2n} \\ & & & \\ & & & \\ & & & \\ C_{n1} & C_{n2} & \cdots & C_{nn} \end{bmatrix} \begin{bmatrix} \omega_{11} \\ \omega_{12} \\ \cdot \\ \cdot \\ \cdot \\ \omega_{1n} \end{bmatrix} \tag{48}$$

where

$$b_j = k \sum_{i=1}^{S} a_{ij} \tag{49}$$

and

$$c_{jk} = \sum_{i=1}^{S} a_{ij}\, (a_{ik} + 1).$$

After a solution to (48) is obtained the second hyperplane, H_2, denoted by its weight vector, $\vec{\omega}_2$, and real number T_2, may be found which minimizes

(51) $$z_2 = \sum_{i=1}^{S} \delta_{2i}^2$$

subject to the constraints that

(52) $$\vec{\omega}_1 \cdot \vec{\omega}_2 = 0$$

where

(53) $$\delta_{2i} = \vec{\omega}_2 \cdot \vec{a}_i - T_2.$$

The constraint given in (52) may be introduced into the problem by introducing the Lagrange multiplier, λ. The problem thus becomes one of minimizing

(54) $$z_2 = \sum_{i=1}^{S} \delta_{2i}^2 + \lambda_1 \vec{\omega}_2 \cdot \vec{\omega}_1.$$

This minimization requires that

(55) $$\frac{\partial z_2}{\partial \omega_{2j}} = 0, \; j = 1, 2, \cdots, n$$

and

(56) $$\frac{\partial z_2}{\partial T_2} = \frac{\partial z_2}{\partial \lambda_1} = 0.$$

Thus

(57) $$0 = \frac{\partial z_2}{\partial \omega_{2j}} = \sum_{i=1}^{S} 2\, a_{ij} (\vec{\omega}_2 \cdot \vec{a}_i - T_2) + \lambda_1\, \omega_{1j}$$

(58) $$0 = \frac{\partial z_2}{\partial T_2} = -\, 2 \sum_{i=1}^{S} (\vec{\omega}_2 \cdot \vec{a}_i - T_2)$$

and

(59) $$0 = \frac{\partial z_2}{\partial \lambda_1} = \vec{\omega}_2 \cdot \vec{\omega}_1 .$$

Again requiring that $\vec{\omega}_2 \cdot \vec{I} + T_2 = k \neq 0$ gives for (57)

(60) $$0 = \sum_{i=1}^{S} 2\, A_{ij} (\vec{\omega}_2 \cdot \vec{a}_i - k + \vec{\omega}_2 \cdot \vec{I}) + \lambda \omega_{ij}$$

$$= \omega_2 \sum_{i=1}^{S} a_{ij} (\vec{a}_i + \vec{I}) - 2\, k \sum_{i=1}^{S} a_{ij} + \lambda_1\, \omega_{1j} \quad .$$

Observe that from (58)

(61) $$T_2 = \vec{\omega}_2 \cdot \vec{\rho}$$

as before. Eqs. (59) and (60) give the problem in matrix form as

$$
(62)\qquad
\begin{bmatrix} b_1 \\ b_2 \\ \cdot \\ \cdot \\ \cdot \\ b_n \\ 0 \end{bmatrix}
=
\begin{bmatrix}
C_{11} & C_{12} & \cdots & C_{1n} & \omega_{11} \\
C_{21} & C_{22} & \cdots & C_{2n} & \omega_{12} \\
 & & \cdots & & \\
 & & \cdots & & \\
 & & \cdots & & \\
C_{n1} & C_{n2} & \cdots & C_{nn} & \omega_{1n} \\
\omega_{11} & \omega_{12} & \cdots & \omega_{in} & 0
\end{bmatrix}
\begin{bmatrix} \omega_{21} \\ \omega_{22} \\ \cdot \\ \cdot \\ \cdot \\ \omega_{2n} \\ \lambda_1 \end{bmatrix}
$$

where

$$
(63)\qquad b_j = 2\,k \sum_{i=1}^{S} a_{ij}
$$

and

$$
(64)\qquad C_{jk} = 2 \sum_{i=1}^{S} a_{ij}\,(a_{ik} + 1).
$$

Continuing in this manner to step ℓ gives

$$
(65)\qquad
\begin{bmatrix} b_1 \\ b_2 \\ \cdot \\ \cdot \\ \cdot \\ b_n \\ 0 \\ 0 \\ \cdot \\ \cdot \\ \cdot \\ 0 \end{bmatrix}
=
\begin{bmatrix}
C_{11} & C_{12} & \cdots & C_{1n} & \omega_{11} & \omega_{21} & \cdots & \omega_{\ell-1,1} \\
C_{21} & C_{22} & \cdots & C_{2n} & \omega_{12} & \omega_{22} & \cdots & \omega_{\ell-1,2} \\
 & & & & \cdot & \cdot & & \cdot \\
 & & & & \cdot & \cdot & & \cdot \\
 & & & & \cdot & \cdot & & \cdot \\
C_{n1} & C_{n2} & \cdots & C_{nn} & \omega_{1n} & \omega_{2n} & \cdots & \omega_{\ell-1,n} \\
\omega_{11} & \omega_{12} & \cdots & \omega_{1n} & 0 & 0 & \cdots & 0 \\
\omega_{21} & \omega_{22} & \cdots & \omega_{2n} & 0 & 0 & \cdots & 0 \\
 & & & & & & & \\
 & & & & & & & \\
 & & & & & & & \\
\omega_{\ell-1,1} & \omega_{\ell-1,2} & \cdots & \omega_{\ell-1,n} & 0 & 0 & \cdots & 0
\end{bmatrix}
\begin{bmatrix} \omega_{\ell 1} \\ \omega_{\ell 2} \\ \cdot \\ \cdot \\ \cdot \\ \omega_{\ell n} \\ \lambda_1 \\ \lambda_2 \\ \cdot \\ \cdot \\ \cdot \\ \lambda_{\ell-1} \end{bmatrix}
$$

where $\ell = 2, 3, \cdots, n$,

(66) $$b_j = 2\ k \sum_{i=1}^{S} a_{ij}$$

and

(67) $$C_{jk} = 2 \sum_{i=1}^{S} a_{ij}\ (a_{ik} + 1)\ .$$

When $\ell = 1$ the first hyperplane may be found from Eq. (48). Furthermore, since k is arbitrary and nonzero it may, without loss of generality, be set equal to one. Note further that

(68) $$T_j = \vec{\omega}_j \cdot \vec{\rho},\ j = 1, 2, \cdots, n.$$

By solving the n problems just described, the face hyperplanes may be found. The actual face positions may be found by locating two hyperplanes parallel to each H_i (their weight vectors will be $\vec{\omega}_i$) such that all of the points in A lie between these hyperplanes. The hyperbox faces are then characterized by the structure $[\vec{\omega}_i;\ T_{iu},\ T_{i\ell}]$, $i = 1, 2, \cdots, n$, where

(69) $$T_{iu} = \underset{j=1,\cdots,S}{\mathrm{Max}} \quad (\vec{\omega}_i \cdot \vec{a}_j)$$

and

(70) $$T_{i\ell} = \underset{j=1,\cdots,S}{\mathrm{Min}} \quad (\vec{\omega}_i \cdot \vec{a}_j) \quad .$$

One measure of the volume of the hyperbox and thus, the clustering of the data is the distance between parallel faces. This distance, d_i, is given by the equation

$$d_i = \frac{T_{iu} - T_{i\ell}}{\sqrt{\sum_{j=1}^{n} \omega_{ij}^2}} \quad . \tag{71}$$

The hyperboxes and corresponding face distances were computed for the data representing the prolate spheroid, the cylinder, the cube, and the hemispherical boss. This information is shown in Tables VI, VII, VIII, and IX respectively. In these tables T1 and T2 correspond to T_{iu} and $T_{i\ell}$ of Eqs. (69) and (70) respectively. T3 represents $\vec{\omega}_i \cdot \vec{\rho}$ and indicates where the box center is with respect to the center of gravity or first moment. If the box center and the center of gravity overlap then T3 = (T1 + T2)/2. D represents the face distances as computed from Eq. (71).

Hyperellipse

A second type of closed hypersurface useful in the classification of target data is the hyperellipse. If such an ellipse has its center at the origin and its axis of symmetry aligned with the coordinate system then the ellipse is defined by

$$d_i\, x_1^2 + d_2\, x_2^2 + \cdots + d_n\, x_n^2 = 1 \quad . \tag{72}$$

Generally the data set, A, will not center on the coordinate origin nor will the point distributions, forming the axis of symmetry, align

PROLATE SPHEROID.

THE HYPERBOX FACES ARE AS FOLLOWS.

W 1	-0.946468	0.737038	-0.188895	-0.662692G-02	0.191321G-01	0.553116G-02
W 2	-1.18004	0.495604G-02	1.96670	0.208234	0.341233	0.158483
W 3	-1.47839	-0.937808G-01	-0.711552	-1.21484	1.54555	-0.115990
W 4	0.603694	0.239647G-01	-0.181930G-01	2.50303	-0.242495	-0.513977
W 5	1.57905	0.791300G-01	0.270293	-3.44494	-0.130337	-0.359584
W 6	2.15847	0.960280G-01	0.122901	3.23543	0.716889	0.156676
W 7	1.75377	0.737339G-01	0.126685	-2.88659	-0.133691G-01	0.288815
W 8	0.742306	0.182308G-01	-0.308532	1.14699	0.198918	0.406775
W 9	-0.346222	-0.293360G-01	-0.416070	0.172713	-0.433507	2.447958
W10	-0.685306	-0.364432G-01	-0.214217	0.414335G-01	-0.862072	0.682271G-01
W11	-0.734835	-0.367434G-01	-0.172643	-0.573954	-0.434869	0.197423
W12	-0.559461	-0.234507G-01	0.343101G-02	1.30707	-0.582572	-0.176920
T 1	0.935663G-01	0.186798	0.540423	0.524979	0.906219	0.477122
T 2	0.933086G-01	0.186547	0.539770	0.506666	0.628356	0.406300
T 3	0.934321G-01	0.186672	0.540091	0.516721	0.877255	0.436242
D	0.624025G-04	0.329644G-03	0.296301G-03	0.283088G-02	0.363252G-01	0.690817G-01

W 1	-0.787129G-03	-0.317605G-03	0.453254G-02	0.168351G-01	-0.748703G-02	0.711899G-01
W 2	-0.136050G-01	0.191448G-02	0.471631G-01	0.553243G-01	0.598193G-01	0.997376G-01
W 3	0.170030G-01	0.126019	0.676042G-01	0.595368G-01	0.773732G-01	0.251111
W 4	-0.135303	-0.702555	0.454342G-01	0.118396	0.116752	0.135421
W 5	0.576223G-01	0.265229	0.961229G-01	0.197265G-01	-0.105001	-0.343796
W 6	0.241827	0.147949	0.212791G-01	-0.420876G-01	-0.121649	-0.188322G-01
W 7	0.404770G-01	-0.199720	-0.342622G-01	-0.203819G-01	0.216612	0.181503
W 8	-0.216342	0.786328	0.279489G-01	0.124777	0.927252G-01	-0.350049
W 9	-0.489926G-02	-0.937044	0.136507	-0.729647G-01	-0.633955G-02	-0.473022G-01
W10	-0.241553G-01	0.998161	0.619969G-01	0.421333G-01	-0.738144G-01	0.537354
W11	0.279158	-0.430891	-0.311837G-01	0.238892	-0.473633G-01	0.236816G-01
W12	0.287367	0.565485	0.325692G-01	-0.585937G-01	0.240234	-0.179687
T 1	0.467507	0.478260	0.848691	0.794207	0.717444	0.728869
T 2	0.364226	0.215118	0.247734	0.963988G-01	0.725344G-01	-0.252431
T 3	0.411962	0.369901	0.416653	0.392936	0.402070	0.311656
D	0.190021	0.137929	2.83174	2.13675	1.56318	1.17770

CENTER OF GRAVITY AT

CG 1	0.241150
CG 2	1.00690
CG 3	1.20121
CG 4	0.833856
CG 5	0.705255
CG 6	0.722667
CG 7	0.676715
CG 8	0.841614
CG 9	0.861209
CG10	0.683649
CG11	0.693459
CG12	0.749878

NOT REPRODUCIBLE

CYLINDER.

THE HYPERBOX FACES ARE AS FOLLOWS.

W 1	0.740194	0.772771	0.938986	-0.603515G-03	-0.106284G-03	0.701989G-04
W 2	-0.624380G-01	1.49175	-0.344185	0.195999	0.539980	0.286370
W 3	-0.345894	-0.962765	0.537447	0.164660G-01	0.326279	0.501956
W 4	0.436928	0.387685G-01	-0.367145	-0.259412	-0.235364	-0.324413G-01
W 5	-0.274641	0.200758	0.171234	0.240436	0.610458G-03	-0.376093
W 6	0.456517	-0.677565	-0.193049	-0.202739	0.533442	-0.100272
W 7	-0.922742G-01	0.350511	-0.171656G-01	0.437392	-0.283056	0.687237G-01
W 8	0.113084	-0.559993	0.568209G-01	0.578468	0.179638G-01	-0.859428G-01
W 9	-0.320929	0.446007	0.126859	-0.322947	-0.359785	0.415968
W10	0.183248	-0.290390	-0.724927G-01	0.116926	-0.272231	0.463010G-01
W11	-0.428007	0.336320	0.259894	-0.280132	0.170299	-0.440912
W12	0.332603	-0.112178	-0.241615	0.805535G-01	0.295429G-01	0.277077
T 1	0.241619	-0.339360G-01	0.144442	0.412116	0.508318	0.483503
T 2	0.241603	-0.340517G-01	0.144382	0.389865	0.435367	0.376550
T 3	0.241611	-0.3399[illegible]-01	0.144412	0.399903	0.478945	0.437593
D	0.130001G-04	0.508880G-04	0.462183G-04	0.230322G-01	0.709954G-01	0.110023
W 1	-0.514236G-04	-0.100237G-03	-0.129501G-03	-0.864646G-04	0.302325G-02	0.356153G-01
W 2	-0.124862	0.183840	-0.[illegible]990G-02	0.171548G-01	0.188320G-01	-0.153892G-01
W 3	-0.868029G-01	-0.818165G-02	0.390751G-01	0.347161G-01	0.508317G-01	-0.161725
W 4	0.370760G-01	0.145994	0.635838G-01	0.713118G-02	0.153511	-0.199265
W 5	-0.281453	-0.834015G-01	0.246537	-0.277178G-01	0.664437G-01	0.495844G-01
W 6	0.345355	0.154296	0.130572	0.563593G-01	-0.508051G-01	0.587661G-01
W 7	0.536413	-0.162328	0.355918G-01	0.923739G-01	-0.592167G-01	-0.124725
W 8	0.242354	0.369796	-0.884091G-01	-0.191176G-01	0.111145	0.964175G-01
W 9	0.258649	0.265730	0.904151G-01	0.569910G-03	0.351925G-01	0.182634
W10	-0.550113	0.257604	0.109781G-01	0.163129	-0.399170G-01	0.444145G-01
W11	0.193129	-0.387812G-01	-0.982819G-01	0.130310	0.771484G-01	0.195312G-02
W12	-0.292755G-01	-0.564677	-0.154686G-01	0.533829G-01	0.104004	0.167236
T 1	0.537132	0.662377	0.783337	0.923790	0.813225	0.918453
T 2	0.345144	0.246707	0.220113	0.204553	0.913287G-01	-0.196239
T 3	0.464438	0.454183	0.495960	0.423088	0.408847	0.283213
D	0.194596	0.494799	1.64798	2.91605	2.74882	2.72234

CENTER OF GRAVITY AT

CG 1	2.190200
CG 2	0.668223
CG 3	0.881119
CG 4	2.750362
CG 5	1.10770
CG 6	1.16418
CG 7	0.684079
CG 8	2.684737
CG 9	1.09862
CG10	3.871513
CG11	4.777369
CG12	0.996546

CUBE.

THE HYPERBOX FACES ARE AS FOLLOWS.

W 1	0.130421G-01	1.04265	0.346697	0.237085G-03	-0.273065G-03	-0.198321G-02
W 2	0.547909	-0.798233G-01	0.178636	-0.152084G-01	0.323147G-02	0.607720G-02
W 3	-0.234466G-01	-0.150267	0.501643	0.227575	-0.255100	-0.490160
W 4	0.570142G-01	0.195416	-0.663815	0.175936	0.815366G-01	0.588340
W 5	-0.355712G-01	-0.883194G-01	0.302749	0.553289G-02	0.646463	0.211463
W 6	-0.294346G-01	-0.213018G-01	0.752818G-01	-0.579519G-01	-0.291042	0.477730G-01
W 7	0.397818G-01	0.863934G-01	-0.296327	0.547989G-01	0.338058	-0.568307
W 8	-0.380277G-01	-0.150268	0.510579	0.395724G-01	0.128415	0.852095
W 9	0.648573G-02	0.507126G-01	-0.169084	-0.435595G-01	-0.127637	0.373900G-03
W10	-0.298392G-02	0.456204G-02	-0.153008G-01	0.834771G-02	0.106353	-0.756866
W11	0.155784G-01	0.276395G-01	-0.940573G-01	0.237758G-01	-0.228787	0.544487
W12	-0.389734G-02	-0.839344G-02	0.280013G-01	-0.363179G-01	0.362414G-01	-0.152021G-01
T 1	0.433663	0.921308G-01	0.295213	0.627263	0.587149	0.690564
T 2	0.433632	0.920329G-01	0.294798	0.607927	0.533817	0.532678
T 3	0.433647	0.922817G-01	0.294997	0.617230	0.561569	0.630125
D	0.591192G-04	0.913640G-04	0.360259G-03	0.628069G-01	0.601530G-01	0.983528G-01

W 1	0.965427G-03	0.401979G-04	0.138982G-02	-0.425978G-02	0.106731G-01	0.179681G-01
W 2	-0.416326G-02	0.876322G-02	0.253087G-02	0.903979G-02	-0.932558G-03	-0.132256G-01
W 3	0.151860	-0.827885G-01	-0.135812G-01	0.390794G-01	0.236752G-01	-0.186577G-01
W 4	-0.579536G-01	0.274986	-0.101665G-01	0.527676G-01	0.470467G-01	-0.288010G-01
W 5	0.812852G-01	-0.193878	0.929275G-01	0.151817	0.406764G-01	-0.626125G-01
W 6	0.164801	0.429277	0.343724	0.885114G-01	0.245653G-01	-0.287852G-01
W 7	0.379150	-0.319012G-01	0.184864	-0.113264	-0.404338G-01	0.101252
W 8	-0.957642G-01	0.280356	0.243307G-01	-0.111361	0.698776G-01	0.101318
W 9	0.215591	-0.242782	-0.368763G-01	0.217052G-01	0.316605	0.376587G-01
W10	-0.538687	0.167596	0.357730G-01	0.107725	0.780296G-01	0.760193G-01
W11	-0.828626G-01	-0.517642	0.124705	0.126776	-0.983543G-01	0.104980
W12	0.347514	0.347798	-0.230176	0.168157	-0.674321G-01	0.686902G-01
T 1	0.586016	0.730696	0.591346	0.695127	0.881792	0.961995
T 2	0.383897	0.385710	0.318639	0.306212	0.954083G-01	0.731095G-01
T 3	0.504650	0.529184	0.462704	0.437107	0.508358	0.460984
D	0.254797	0.370877	0.564943	1.13725	2.16269	3.86072

CENTER OF GRAVITY AT

CG 1	0.176555
CG 2	0.719873
CG 3	1.38896
CG 4	1.50562
CG 5	0.871279
CG 6	0.661828
CG 7	1.35456
CG 8	1.53337
CG 9	1.19947
CG10	1.27118
CG11	1.20898
CG12	0.961246

HEMI-SPHERICAL [illegible] S.

THE HYPERBOX FACES ARE AS FOLLOWS.

W 1	1.21994	-12.1399	-0.769222G-01	-0.178374	1.76124	2.442879
W 2	0.35119[illegible]	18.8502	1.46816	0.389228G-01	-1.29268	0.318276
W 3	-0.3521[illegible]G-01	21.4341	-0.231172	0.638258	2.44849	0.289[illegible]
W 4	-0.933977	-18.2140	-0.313748	0.123739	-0.226547	0.63[illegible]
W 5	0.7349[illegible]7G-01	-13.7603	0.734978	0.368495	0.677285	-2.995337
W 6	0.50[illegible]	-6.09559	-0.456873	0.185558	-1.41741	2.027254
W 7	-0.42607[illegible]G-[illegible]	2.97726	0.239678	0.213216	-2.51438	-0.162851
W 8	0.14[illegible]	-3.64337	-0.963427	0.995128G-01	2.44752[illegible]	-2.35833[illegible]
W 9	-0.276[illegible]43	-13.0363	1.25516	-0.134252	1.57463	0.3356[illegible]
W10	0.73[illegible]49G-01	17.7002	-2.527224	-0.330307	-0.144423	-2.252805
W11	0.23807[illegible]	-5.23983	-0.116709	0.224572	-1.27[illegible]98	2.151839
W12	-0.164646	8.49717	0.158399G-03	-0.314199	0.915139	-2.514221G-01
T 1	0.1752[illegible]G-01	-2.414357	-0.1[illegible]2G-01	2.150735G-01	-0.825966	0.787425G-02
T 2	0.174442G-01	-2.411633	-0.184425G-01	0.153461G-01	-0.628363	2.68143[illegible]G-02
T 3	0.174[illegible]4G-01	-2.412666	-0.133547G-01	0.[illegible]5856G-01	-0.8268376	0.7506[illegible]4G-02
D	0.39[illegible]3[illegible]G-04	0.289264G-04	0.979818G-04	0.282169G-04	0.5[illegible]G-[illegible]	0.665956G-03

W 1	0.682620	0.116173	-0.291186G-01	2.113162G-02	-0.393535G-01	-0.4[illegible]8667
W 2	-2.53187[illegible]G-01	0.778994	-2.493387G-01	0.189375G-02	0.121269	2.262864
W 3	0.5015[illegible]G-01	-0.257809	-0.108497G-01	-0.663567G-02	-2.807571G-01	0.927734G-01
W 4	0.483482	0.559514	0.414307	0.372314G-02	-0.971680G-01	-0.525[illegible]G-01
W 5	0.114629	0.231594	0.834160	0.129811	-0.213[illegible]51	-0.129883
W 6	-0.499687	-0.144347	1.11838	0.252263	0.128883	0.231689
W 7	0.650723	-0.496181	-0.24873[illegible]	0.146296	0.446533	-0.625[illegible]G-01
W 8	-0.263855	0.712493	-0.574259	0.225830G-01	0.556274	0.[illegible]
W 9	-0.277548	-2.377229	-0.861597G-02	-0.131313	0.387451	0.113281
W10	0.293271	-2.412266G-01	0.956516	-0.337648	-2.115356	0.351562G-01
W11	-0.129625	-0.86[illegible]453G-01	-0.944677	-0.161139	-0.621918	0.141602
W12	0.383254G-01	-0.243582G-01	-0.242981	0.670446	-0.252350	0.195312G-01
T 1	-0.602963G-02	-0.927758G-03	-0.141482	0.523432	0.993301	1.14325
T 2	-0.611577G-02	-0.324686G-02	-0.249536	0.182302	0.998692G-01	0.633861G-01
T 3	-0.60813[illegible]G-02	-0.169991G-02	-0.212721	0.407832	0.688823	0.548545
D	0.68066[illegible]G-04	0.160571G-02	0.516349G-01	0.383933	0.811485	1.82584

CENTER OF GRAVITY AT

CG 1	0.590184G-01
CG 2	0.199043
CG 3	0.335632
CG 4	0.388146
CG 5	0.390559
CG 6	0.642045
CG 7	1.18989
CG 8	1.68207
CG 9	1.82218
CG10	1.67226
CG11	1.09425
CG12	1.47850

with the coordinate axis. Under these circumstances the ellipse will be described by

$$(\vec{x} - \vec{\beta})\ P\ (\vec{x} - \vec{\beta})^T = 1, \tag{73}$$

where $\vec{\beta}$ is the ellipse center and P is the matrix describing the ellipse orientation. The problem now becomes one of estimating the parameters $\vec{\beta}$ and P for an ellipse which completely encloses the data set.

One easily obtainable estimation of these parameters may be made on the basis of the location and orientation of the hyperboxes described above. The center of the ellipse may be aligned with the center of the hyperbox or with the center of gravity of the data set. Call this center $\vec{\xi}$. Then a new coordinate system may be found by moving the old coordinate system origin to the $\vec{\xi}$ thus forming the data set

$$A' = \{a_1', \cdots, a_s'\} \tag{74}$$

where

$$\vec{a}_i' = \vec{a}_i - \vec{\xi}. \tag{75}$$

The orientation of the ellipse may reasonably be choosen to coincide with the hyperbox described above. Letting $\vec{\omega}_1, \cdots, \vec{\omega}_n$ be the ordered set of hyperplanes found for the hyperbox, the unit vectors describing a basis for a rotated coordinate system aligned with these vectors become

(76) $\vec{\omega}_i^* = \vec{\omega}_i / \left\| \vec{\omega}_i \right\|, \; i = 1, 2, \cdots, n.$

Thus, the data set in this rotated space becomes

$$A'' = \{\vec{a}_1'', \cdots, \vec{a}_s''\}$$

where

(77) $(\vec{a}_i')^T = W(\vec{a}_i'')^T$

for

(78) $$W = \begin{bmatrix} \vec{\omega}_1^* \\ \vec{\omega}_2^* \\ \cdot \\ \cdot \\ \cdot \\ \vec{\omega}_n^* \end{bmatrix} .$$

Thus, since W is nonsingular

(79) $(\vec{a}_i'')^T = W^{-1} (\vec{a}_i')^T.$

Thus, an ellipse circumscribing the data set A" has a defining equation of the form of Eq. (72).

For an ellipse to circumscribe this data it is necessary that

(80) $\vec{d} \cdot \vec{V}_i - 1 \leq 0, \; i = 1, 2, \cdots, S$

where

$$\vec{d} = (d_1, d_2, \cdots, d_n)$$

and

(81) $$\vec{V}_i = (a_{i1}^{''2}, a_{i2}^{''2}, \cdots, a_{in}^{''2}).$$

The determination of d from inequalities (80) will thus specify the ellipse.

This problem may now be stated as a linear programing problem by modifying (80) to

(82) $$\vec{d} \cdot \vec{V}_i + S_i = 1, i = 1, 2, \cdots, S$$

subject to the constraints that

(83) $$d_j \geq 0, j = 1, 2, \cdots, n$$

and

(84) $$S_i \geq 0, i = 1, 2, \cdots, S.$$

Since the smallest ellipse is required an appropriate objective function is the minimization of

(85) $$z = \sum_{i=1}^{S} S_i.$$

Upon solving this linear programming problem the coordinate system may be transferred back to the original system as follows. Let

(86) $$D = \begin{bmatrix} d_1 & & & & 0 \\ & d_2 & & & \\ & & \cdot & & \\ & & & \cdot & \\ & & & & \cdot \\ 0 & & & & d_n \end{bmatrix} .$$

Then the equation of the ellipse becomes

(87) $$1 = \vec{x}'' \, D \, (\vec{x}'')^T$$

but

(88) $$(\vec{x}'')^T = W^{-1}(\vec{x}')^T$$

$$= W^{-1}(\vec{x} - \vec{\xi})^T$$

or

(89) $$1 = (\vec{x} - \vec{\xi}) \, (W^{-1})^T \, D \, W^{-1}(\vec{x} - \vec{\xi})^T.$$

Thus, the enclosing ellipse for each object class is specified by the set of parameters ξ, W^{-1}, and D.

CONCLUSIONS

A study of the identification of targets using their frequency responses has been carried out. The objects considered for classification were represented by a set of points in a twelve dimensional Euclidean space corresponding to the twelve test frequencies. Only one object was completely symmetrical and thus represented by a single point. Some of the other objects considered, e.g., a spheroid, cube, hemispherical boss, provided a different return depending on the aspect angle. Thus each object was usually represented by a set of points scattered over a portion of the twelve-space. The first and most important fact to ascertain was whether the classes were separable. The investigation revealed that indeed all classes considered were separable, moreover each class was linearly separable from all other classes.

A very interesting and useful fact was discovered in the process of constructing the hyperplanes separating the various classes. It was found that the average number of non zero components of the separating vector was three. It thus appears that the dimensionality of the feature extraction process may be substantially reduced from the twelve that was originally postulated. The implications of this discovery with respect to the reduction in the equipment complexity required for system implementation are quite obvious.

In order to test the reliability of detection based on the separating hyperplanes, substantial amount of additional data were obtained covering new aspect angles for the various objects considered.

These data were used as test data as compared to the first data which constituted the training sets. The results of the test showed that all test data used were correctly identified.

A study was also carried out into the effects of noise on the separability of the classes considered. The effects of noise on both training sets and test sets were studied. The results indicate that when the training sets were noise free the system would correctly identify noisy test sets up to noise levels of the order of 10 percent of the signal. With regard to noisy training sets, it was shown that class separability was possible up to noise levels of 50% of signal, indicating that an adaptive classifier may be very beneficial for situations where the training samples are either noisy or the population incompletely known. One such adaptive procedure has been developed and found to converge quite rapidly, in most cases four iterations or less were adequate.

An automatic target classifier has been developed and successfully tested on various objects. The target responses used were contaminated by noise to varying degrees. The results have indicated that a high probability of correct classification could be obtained up to moderate amounts of noise and measurement errors.

A technique has been devised to determine target dynamics, such as the rotation axis of a satellite, based on its vector trajectory in n space.

A study has been carried out of the use of nonlinear separating hypersurfaces for classification of objects that may not be linearly separable. Two types of closed surfaces have been used, hyperboxes and hyperellipsoids. The use of these surfaces led to an assessment of the clustering properties of the various objects studied. It was found that the object classes examined were tightly packed and occupied extremely small volumes.

Further work in assessing the resolvability of new objects and the distribution of their representative point classes is continuing.

APPENDIX A

INTERPOLATION ALGORITHM

The interpolation of the backscatter data requires interpolating twelve functions of aspect angle one for each of the illuminating frequencies. There are, of course, many procedures which may be used to accomplish such interpolation. In virtually all cases, a very large system of equations must be solved in order to determine some approximating function or spline fit. Furthermore, each system of data requiring interpolation has a variable range of aspect angles to be considered. Because of these things a local interpolation procedure was desired.

Consider the situation shown in Fig. A1. The function f(x) has been specified by its values at $x = x_0, x_1, \cdots, x_n$. A particularly straight forward way of interpolating f(x) is to connect adjacent points, say $f(x_i)$ and $f(x_{i+1})$, by sections of one or more quadratics.

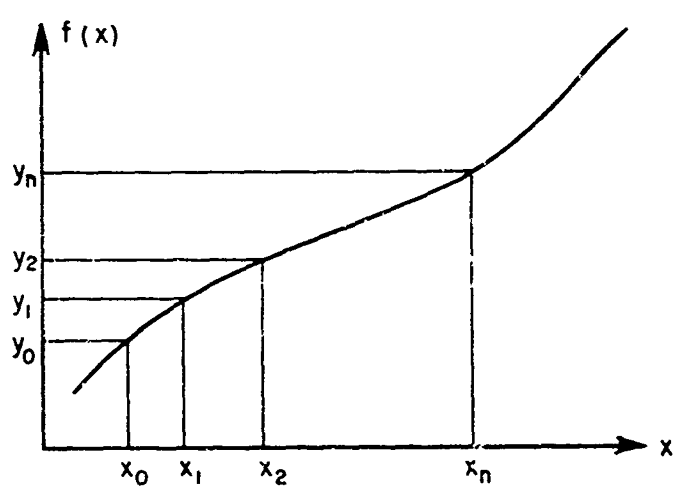

Fig. A1. Interpolation schema.

In particular consider the values of the function at the points x_{i-1}, x_i, and x_{i+1}. Call the functional value y_{i-1}, y_i and y_{i+1} respectively. These three points may then be used to describe a quadratic of form

(A1) $$y = a_{i1} x^2 + a_{i2} x + a_{i3}$$

which is defined by

(A2) $$\begin{bmatrix} y_{i-1} \\ y_i \\ y_{i+1} \end{bmatrix} = \begin{bmatrix} x_{i-1}^2 & x_{i-1} & 1 \\ x_i^2 & x_i & 1 \\ x_{i+1}^2 & x_{i+1} & 1 \end{bmatrix} \begin{bmatrix} a_{i1} \\ a_{i2} \\ a_{i3} \end{bmatrix}$$

for i = 1, 2, ···, n-1. A solution to (A2) will produce a quadratic approximation of f(x) given by (A1) for the range $x_{i-1} \leq x \leq x_{i+1}$. Because a solution to (A2) for all i in the specified range is straight forward a better approximation may be made as follows:

(A3) $$y = a_{11} x^2 + a_{12} x + a_{13}, \quad x_o \leq x \leq x ,$$

(A4) $$y = \frac{a_{i-1,1} + a_{i,1}}{2} x^2 + \frac{a_{i-1,2} + a_{i,2}}{2} x + \frac{a_{i-1,3} + a_{i,3}}{2} ,$$

$$x_{i-1} \leq x \leq x_i, \quad i = 2, 3, \cdots, n - 1$$

and

(A5) $$y = a_{n-1,1} x^2 + a_{n-1,2} x + a_{n-1,3}, \quad x_{n-1} \leq x \leq x_n.$$

This approximation, effectively, is an average of two quadratics for all x outside of the ranges from x_0 to x_1 and x_{n-1} to x_n. Since the data used here is well behaved in the sense that the first and second derivatives are small, the lack of slope matching at the approximation boundaries should not appreciably affect the interpolation.

The appropriate coefficients required by (A3), (A4), and (A5) may be found from Eq. (A2) after making some appropriate assumptions. Since the aspect angles for the data were taken in equal steps, assume that $x_i = x_0 + i\delta$ where δ is the spacing increment. Finally, without loss of generality, it may be assumed that $x_0 = 0$. Thus, solving (A2) yields

$$a_{i1} = \frac{y_{i-1} - 2y_i + y_{i+1}}{2\delta^2} \tag{A6}$$

$$a_{i2} = \frac{-(2i + 1)\, y_{i-1} + 4i y_i - (2i - 1)\, y_{i+1}}{2\delta} \tag{A7}$$

$$a_{i3} = \frac{i(i + 1)\, y_{i-1} - 2(i^2 - 1)\, y_i + i(i - 1)\, y_{i+1}}{2} \tag{A8}$$

for $i = 1, 2, \cdots, n-1$.

APPENDIX B

BACKSCATTERED DATA

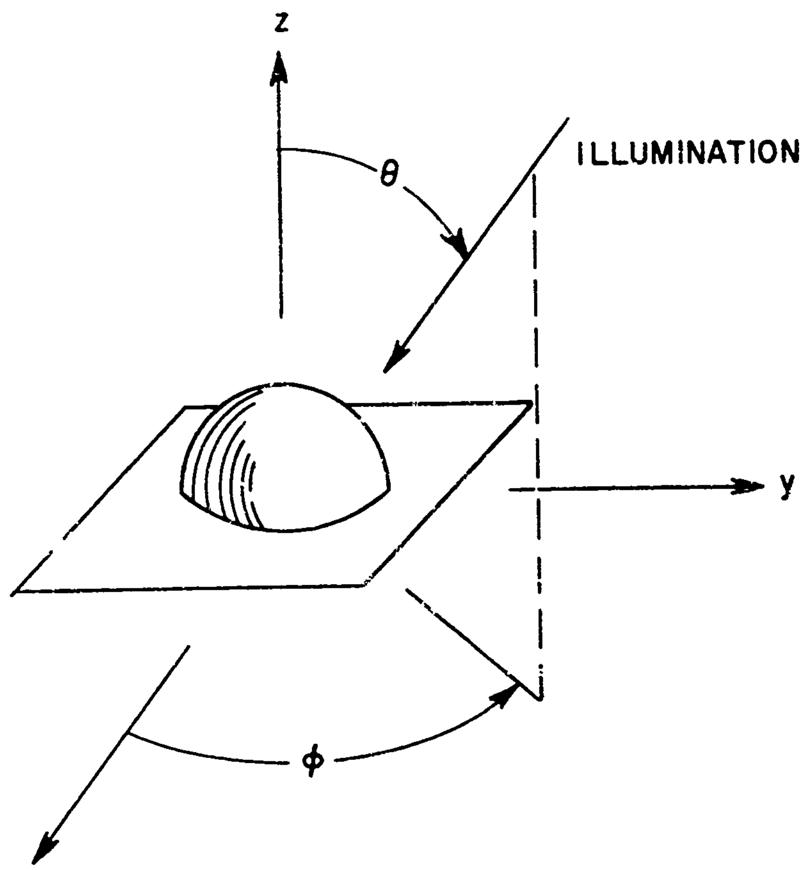

HEMI–SPHERICAL BOSS
DIAMETER = 0.795 M

θ / f(MHz)	Polarization = $\hat{\phi}$ Magnitude				
	15°	30°	45°	60°	75°
30	.111	.089	.059	.029	.008
60	.385	.302	.195	.094	.025
90	.687	.519	.317	.145	.037
120	.883	.621	.340	.137	.030
150	.938	.608	.320	.148	.041
180	1.182	.901	.653	.372	.108
210	2.037	1.712	1.260	.677	.186
240	3.026	2.501	1.736	.862	.222
270	3.574	2.826	1.803	.791	.187
300	3.604	2.667	1.477	.502	.084
330	3.294	2.271	1.125	.459	.151
360	2.876	2.063	1.378	.887	.290
	Phase				
30	.298	.274	.353	-.32	.37
60	2.203	2.187	2.249	2.273	2.097
90	7.141	7.646	8.283	8.972	11.08
120	17.2	19.61	23.9	29.695	34.44
150	39.1	50.18	71.24	96.12	112.53
180	77.0	97.66	120.02	133.92	140.22
210	100.73	117.54	132.3	140.84	144.94
240	106.38	121.61	134.24	141.28	144.44
270	108.1	124.44	137.39	144.44	147.63
300	111.65	131.97	149.26	164.16	-177.61
330	118.67	148.5	-176.57	-126.29	-92.82
360	129.35	175.07	-133.54	-95.92	-81.37

HEMI-SPHERICAL BOSS

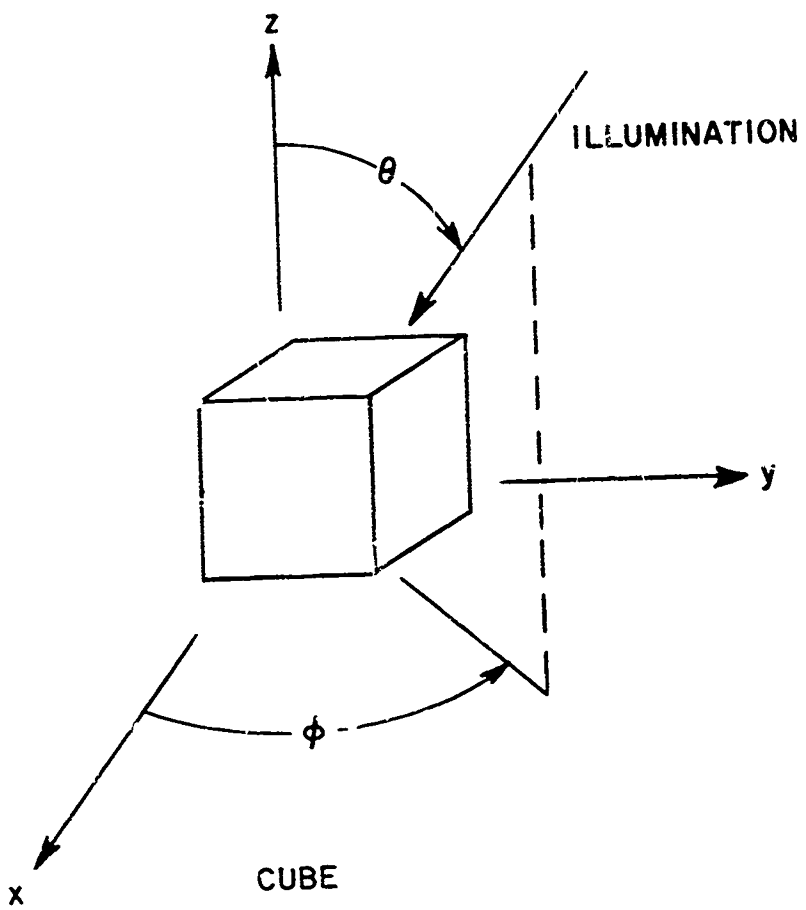

CUBE

EDGE LENGTH = 0.682 M

θ,φ / f(MHz)	Polarization = $\hat{\phi}$ Magnitude									
	0,0	15,0	30,0	45,0	15,45	30,45	45,45	60,45	75,45	90,45
30	.176	.176	.176	.176	.177	.177	.177	.177	.177	.177
60	.706	.706	.706	.706	.707	.717	.732	.748	.748	.748
90	1.33	1.33	1.33	1.33	1.408	1.393	1.434	1.459	1.505	1.49
120	1.483	1.371	1.417	1.371	1.454	1.46	1.587	1.69	1.731	1.7
150	.624	.65	.701	.734	.64	.778	.983	1.193	1.352	1.418
180	.813	.685	.486	.386	.671	.369	.461	.881	1.065	1.085
210	2.128	1.903	1.437	1.197	1.92	1.357	.814	.722	.835	.886
240	2.68	2.179	1.448	1.089	2.355	1.679	1.05	.804	.891	.947
270	2.419	1.811	.644	.121	2.227	1.562	.922	.722	.881	.998
300	2.179	1.693	.691	.716	1.853	1.147	.553	.41	.737	.973
330	1.826	1.627	.916	1.028	1.628	.916	.404	.154	.594	1.0
360	1.836	1.376	.89	.921	1.674	.886	.456	.302	.471	1.08
	Phase									
30	0	0	0	0	0	0	0	0	0	0
60	-4	-5	-5.5	-6	-8	-8	-8	-9	-8	-8
90	-17	-17	-18	-18	-18	-18	-18	-18	-17	-17
120	-34	-32	-35	-34	-34	-34	-33	-33	-32	-32
150	-32.5	-34	-37	-39	-35	-37	-37	-36	-34	-31
180	103	95	96	74	97	71	2	-20	-21	-20
210	97	88	89	86	94	88	65	24	9	7
240	96	90	80	58	75	88	72	43	30	28
270	106	110	100	22	102	92	74	43	29	26
300	126	-232	168	-142	122	108	85	35	13	9
330	155	-206	194	-142	150	137	136	79	-17	-19
350	161	-190	202	-126	180	161	148	158	-39	-35

CUBE

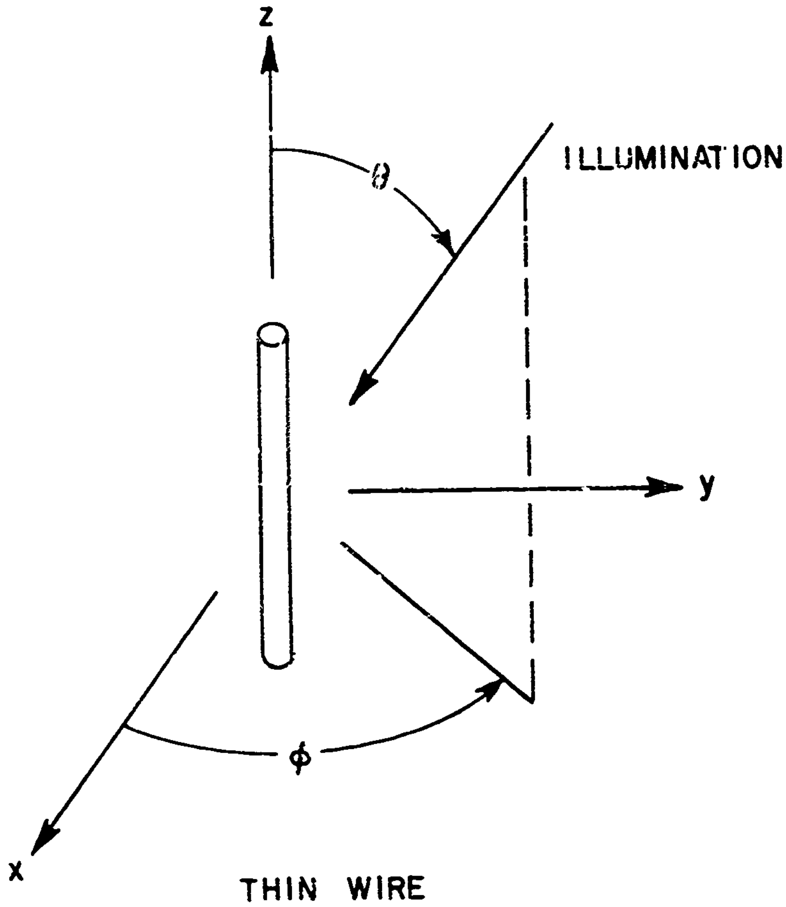

THIN WIRE

DIAMETER = 5 cm

LENGTH = 1 M

θ / f(MHz)	Polarization = $\hat{\theta}$ Magnitude 30°	90°
30	.002	.009
60	.009	.042
90	.031	.153
120	.084	.460
150	.08	.466
180	.056	.316
210	.059	.253
240	.092	.227
270	.139	.211
300	.112	.198
330	.093	.186
360	.10	.172
	Phase	
30	0	0
60	358	358
90	349	349
120	312	314
150	236	241
180	210	223
210	191	219
240	163	218
270	111	219
300	60	221
330	34	224
360	6.6	234

THIN WIRE

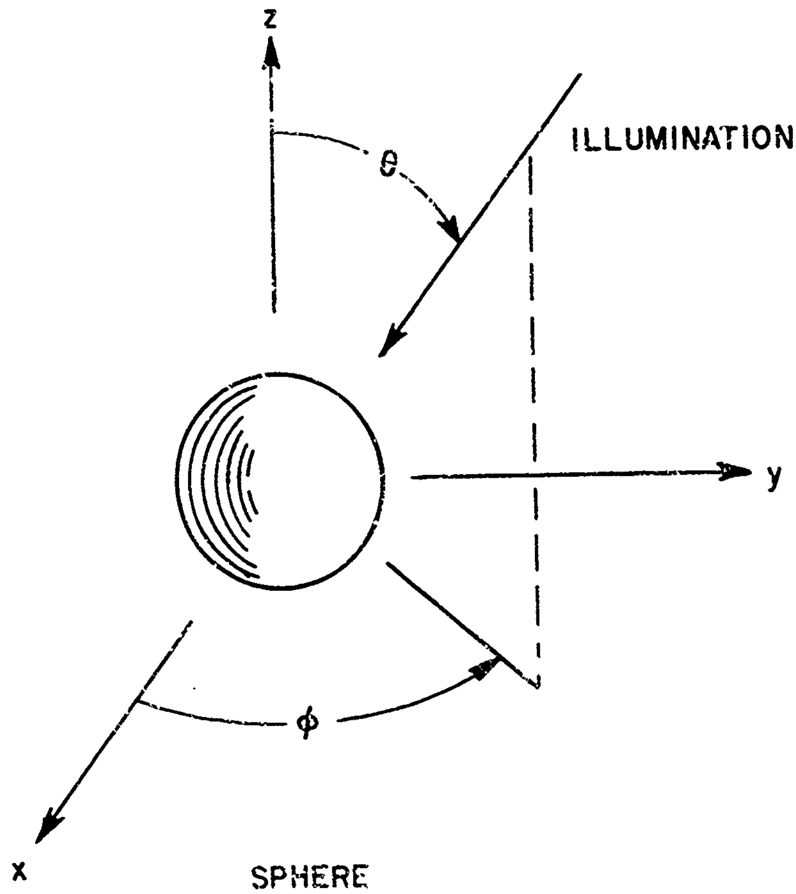

SPHERE

size / f(MHz)	Magnitude		
	d = 1m cond.	d = 0.6m cond.	d = .637m ε_r = 2.208
30	.26	.057	.013
60	.983	.223	.05
90	1.66	.488	.107
120	1.47	.792	.175
150	.74	.394	.237
180	.652	.986	.269
210	1.184	.809	.242
240	1.15	.539	.153
270	.713	.299	.143
300	.771	.391	.29
330	1.09	.614	.387
360	1.02	.736	.394
	Phase		
30	359	0	0
60	354	359	359
90	340	355	357
120	332	349	354
150	347	340	347
180	76	333	336
210	98	332	318
240	108	340	280
270	139	17	182
300	204	76	128
330	231	93	99
360	249	100	72

SPHERE

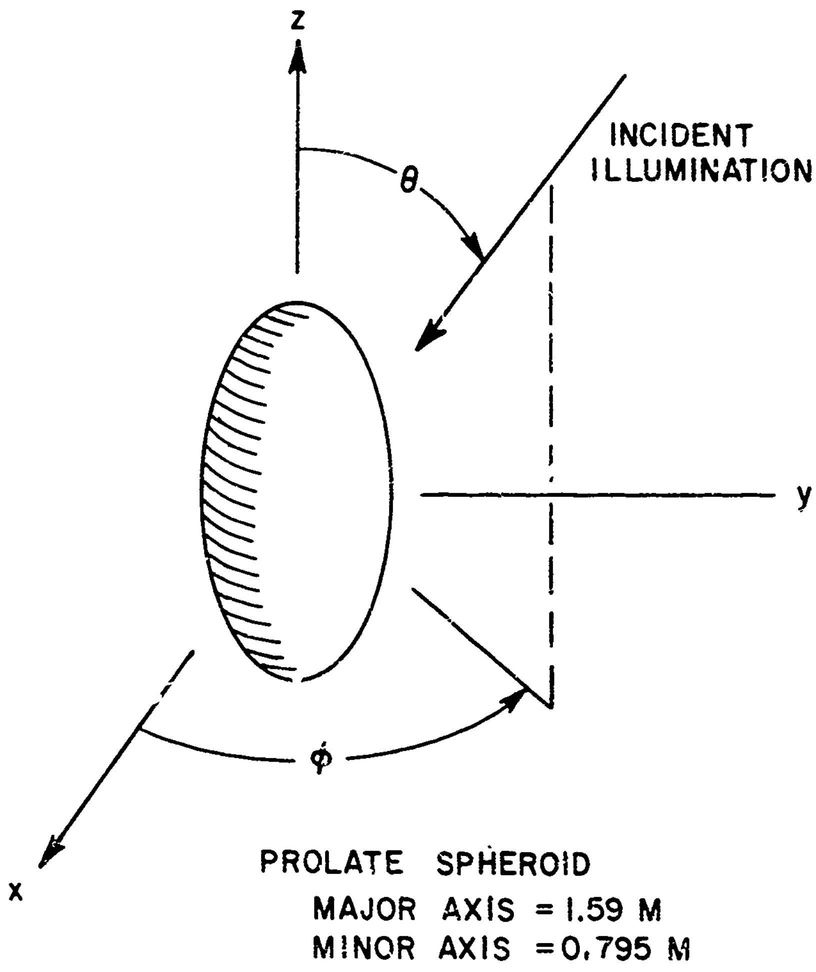
z
INCIDENT
ILLUMINATION
θ
y
φ
x
PROLATE SPHEROID
MAJOR AXIS = 1.59 M
MINOR AXIS = 0.795 M

θ / f(MHz)	0°	10°	20°	30°	40°	50°	60°	70°	80°	90°
	Polarization = $\hat{\phi}$									
	Magnitude									
30	.225	.226	.228	.231	.236	.241	.247	.254	.261	.264
60	.66	.678	.711	.74	.806	.902	1.073	1.324	1.57	1.679
90	.618	.658	.738	.869	.964	1.104	1.325	1.65	2.009	2.179
120	.083	.064	.074	.214	.573	.827	1.131	1.509	1.905	2.093
150	.643	.623	.552	.414	.232	.267	.592	.993	1.38	1.559
180	.654	.684	.753	.807	.79	.675	.549	.605	.815	.933
210	.009	.054	.234	.5	.782	.976	1.034	1.023	1.033	1.05
240	.618	.59	.482	.25	.26	.720	1.123	1.381	1.533	1.59
270	.544	.59	.687	.718	.547	.323	.758	1.297	1.678	1.822
300	.114	.073	.236	.559	.802	.738	.523	.887	1.397	1.61
330	.592	.568	.445	.187	.492	.9	.915	.772	.994	1.175
360	.438	.501	.612	.626	.339	.584	1.074	1.146	1.086	1.103
	Phase									
30	.79	1	1.95	3.7	6.35	9.66	13.16	16.6	18.7	18.3
60	-6.2	-6.1	-5.6	-4.96	-13.5	-16.8	-18.2	-16.9	-15	-16.15
90	-16.8	-16.9	-17	-15.4	-14.5	-14.9	-16.1	-17.4	-18.8	-22.6
120	111	95.6	21	-10.3	-9.76	-6.38	-5.79	-7.56	-11.1	-17.1
150	154	154	153	149	124	48.9	23.7	14.7	7.12	-1.53
180	144	145	147	149	149	142	119	81.1	54.5	39.2
210	-3.93	143	149	152	155	157	153	141	123	107
240	-48.2	-48.4	-50.1	-65.1	-170	172	170	164	154	140
270	-51.2	-50.7	-49.7	-49.1	-55.1	-112	-164	-173	174	160
300	86.8	43.4	-33.5	-41.7	-41.8	-47.1	-88.9	-141	-161	-179
330	111	111	106	62.7	-22.9	-29.3	-38	-74.4	-118	-144
360	117	116	114	111	83.3	-3.2	-15.6	-29.7	-59.1	-88

PROLATE SPHEROID

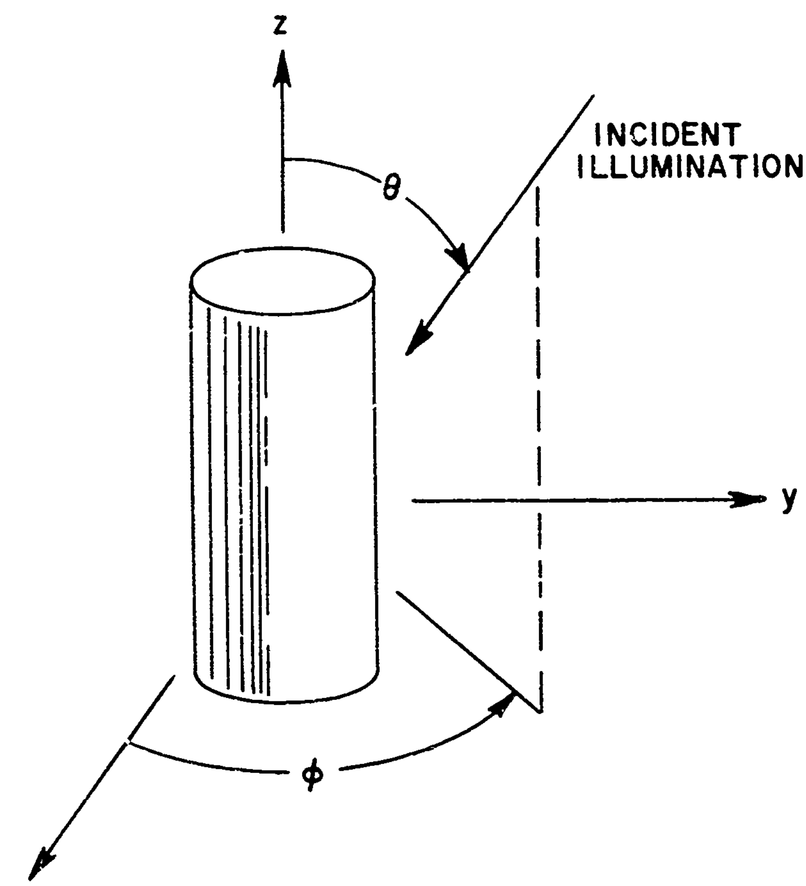

CYLINDER

DIAMETER = 0.635 M
LENGTH = 1.27 M

θ / f(MHz)	Polarization = $\hat{\phi}$									
	0°	10°	20°	30°	40°	50°	60°	70°	80°	90°
30	.19	.19	.19	.19	.19	.19	.19	.19	.19	.19
60	.61	.55	.63	.53	.55	.65	.61	.67	.86	.99
90	.43	.46	.47	.47	.63	.81	.93	1.08	1.32	1.5
120	.41	.37	.28	.15	.16	.54	.91	1.29	1.72	1.87
150	1.43	1.41	1.34	1.16	.8	.34	.38	1.0	1.61	1.89
180	1.28	1.31	1.38	1.43	1.28	.96	.5	.72	1.32	1.61
210	.11	.09	.32	.69	.93	.94	.72	.68	1.07	1.33
240	1.65	1.54	1.18	.63	.29	.44	.54	.70	.99	1.15
270	1.92	1.86	1.62	1.21	.79	.41	.17	.53	1.25	1.55
300	.97	.99	1.01	.93	.77	.63	.45	.13	1.19	1.99
330	1.28	1.14	.76	.42	.19	.36	.56	.30	1.18	2.10
360	2.07	1.89	1.33	.79	.45	.12	.46	.44	1.05	1.93

CYLINDER

REFERENCES

1. Lewis, R. M., Physical Optics Inverse Diffraction, IEEE Trans. on Antenna and Propagation, Vol. AP-17, May 1969, pp. 308-317.

2. Kennaugh, E. M., Moffatt, D. L., and Schafer, R. C , "Final Report - Research into the Scattering of Electromagnetic Energy from highly Conducting Bodies," The Ohio State University ElectroScience Laboratory, Report 1793-4, 24 May 1967; prepared under Contract AF 19(628)-4002 for Air Force Cambridge Research Laboratories, Bedford, Massachusetts.

3. Kennaugh, E. M., Moffatt, D. L., Transient and Impulse Response Approximations, Proc. IEEE. Vol. 53, August 1965, pp. 893-901.

4. Gass, S. I., Linear Programming, McGraw-Hill, 2nd edition, New York, 1964.

5. Muroga, S., Threshold Logic, Class notes, Department of Computer Science, University of Illinois, Urbana, Illinois, 1967.

6. Iburaki and Muroga, S., "Adaptive Linear Classifier by Linear Programming," Report 284, Department of Computer Science, University of Illinois, Urbana, Illinois, September 1968.

7. Lewis II, P. M., and Coats, C. L., Threshold Logic, Ch. 10, John Wiley and Sons, New York 1967.

8. Agnon, S., "The Relaxation Method of Linear Inequalities," Con. J. of Math., 6, pp. 382-392, 1954.

9. Ho, Y. C. and Koshyap, R. L., "An Algorithm for Linear Inequalities and its Applications," IEEE TEC, EC-14, No. 5, pp. 683-688, October 1965.

Security Classification

DOCUMENT CONTROL DATA - R & D

(Security classification of title, body of abstract and indexing annotation must be entered when the overall report is classified)

1. ORIGINATING ACTIVITY (Corporate author)
The Ohio State University
ElectroScience Laboratory
Columbus, Ohio 43212

2a. REPORT SECURITY CLASSIFICATION
UNCLASSIFIED

2b. GROUP

3. REPORT TITLE

THE INVERSE SCATTERING AND TARGET IDENTIFICATION PROBLEM

4. DESCRIPTIVE NOTES (Type of report and inclusive dates)
Scientific Interim

5. AUTHOR(S) (First name, middle initial, last name)

K. J. Breeding
A. A. Ksienski

6. REPORT DATE
4 November 1970

7a. TOTAL NO. OF PAGES
67

7b. NO. OF REFS
9

8a. CONTRACT OR GRANT NO.
AFOSR 69-1710

b. PROJECT NO. 9769

c. 61102F

d. 681304

9a. ORIGINATOR'S REPORT NUMBER(S) TR 2768-4

9b. OTHER REPORT NO(S) (Any other numbers that may be assigned this report)
AFOSR 70-2780TR

10. DISTRIBUTION STATEMENT

1. This document has been approved for public release and sale; its distribution is unlimited.

11. SUPPLEMENTARY NOTES

TECH OTHER

12. SPONSORING MILITARY ACTIVITY
Air Force Office of Scientific Research (NM)
1400 Wilson Blvd
Arlington, Virginia 22209

13. ABSTRACT

In order to obtain an exact solution to the inverse scattering problem, the target response is required over a continuous band of frequencies and aspect angles. An alternative approach to the problem which requires a much more modest amount of measurement data but assumes substantial a priori information is as follows: A finite set of alternatives is specified regarding target shape and composition and a set of measurements is carried out to provide the answer as to which one of the alternatives holds. Since it is necessary to restrict the measurements to a relatively small range of frequencies the question arises as to what frequency band is best to characterize the target and to provide the most reliable discrimination from other targets. The best apparent choice is the highest frequency possible since for a given percent bandwidth it would contribute the greatest amount of information. However, an examination of the Fourier transform of the impulse response indicated that the frequency range corresponding to wavelengths starting with the size of the object and increasing to ten times its dimension would provide the most useful initial information. It is low frequency range which is used in this paper to characterize the various objects of interest, and provides the information used to identify the objects.

DD FORM 1 NOV 65 1473

Security Classification